

Article

Protein-induced Change in Ligand Protonation during Trypsin and Thrombin Binding: Hint on Differences in Selectivity Determinants of both Proteins?

Khang Ngo, Chelsey Collins-Kautz, Stefan Gerstenecker, Björn Wagner, Andreas Heine, and Gerhard Klebe

J. Med. Chem., **Just Accepted Manuscript** • DOI: 10.1021/acs.jmedchem.9b02061 • Publication Date (Web): 03 Feb 2020

Downloaded from pubs.acs.org on February 10, 2020

Just Accepted

"Just Accepted" manuscripts have been peer-reviewed and accepted for publication. They are posted online prior to technical editing, formatting for publication and author proofing. The American Chemical Society provides "Just Accepted" as a service to the research community to expedite the dissemination of scientific material as soon as possible after acceptance. "Just Accepted" manuscripts appear in full in PDF format accompanied by an HTML abstract. "Just Accepted" manuscripts have been fully peer reviewed, but should not be considered the official version of record. They are citable by the Digital Object Identifier (DOI®). "Just Accepted" is an optional service offered to authors. Therefore, the "Just Accepted" Web site may not include all articles that will be published in the journal. After a manuscript is technically edited and formatted, it will be removed from the "Just Accepted" Web site and published as an ASAP article. Note that technical editing may introduce minor changes to the manuscript text and/or graphics which could affect content, and all legal disclaimers and ethical guidelines that apply to the journal pertain. ACS cannot be held responsible for errors or consequences arising from the use of information contained in these "Just Accepted" manuscripts.

Protein-induced Change in Ligand Protonation during Trypsin and Thrombin Binding: Hint on Differences in Selectivity Determinants of both Proteins?

Khang Ngo[†], Chelsey Collins-Kautz[†], Stefan Gerstenecker[†], Björn Wagner[‡], Andreas
Heine[†], Gerhard Klebe^{*†}

[†]Institute of Pharmaceutical Chemistry, Philipps-University Marburg, Marbacher Weg 6,
35032 Marburg, Germany

[‡]Pharma Research Non-Clinical Safety, F. Hoffmann-La Roche AG, 4070 Basel
(Switzerland)

ABSTRACT

Trypsin and thrombin, structurally similar serine proteases, recognize different substrates; thrombin cleaves after Arg whereas trypsin after Lys/Arg. Both recognize basic substrate headgroups via Asp189 at the bottom of the S1-pocket. By crystallography and ITC, we studied a series of D-Phe/-D-DiPhe-Pro-(amino)pyridines.

1
2
3
4 Identical ligand pairs show the same binding poses. Surprisingly, one ligand binds to
5
6
7 trypsin in protonated, to thrombin in unprotonated state at P1 along with differences in the
8
9
10 residual solvation pattern. While trypsin binding is mediated by an ordered water
11
12
13 molecule, in thrombin water is scattered over three hydration sites. Although having highly
14
15
16 similar S1-pockets, our results suggest different electrostatic properties of Asp189
17
18
19 possibly contributing to the selectivity determinant. Thrombin binds a specific Na⁺-ion next
20
21
22 to Asp189 which is absent in trypsin. The electrostatic properties across the S1-pocket
23
24
25 are further attenuated by charged Glu192 at the rim of S1 in thrombin which is replaced
26
27
28 by uncharged Gln192 in trypsin.
29
30
31
32
33
34
35
36

37
38 Keywords: Trypsin & Thrombin, Selectivity, Protonation States, Isothermal Titration
39
40 Calorimetry, X-ray Crystallography, Protein-Ligand Interactions
41
42
43
44
45
46
47
48
49
50
51
52
53
54
55
56
57
58
59
60

INTRODUCTION

The success of a drug molecule in therapy strongly depends on its selectivity profile toward a given protein target. Experience shows that in some cases high selectivity is the prerequisite for an effective therapy without unwanted side effects, whereas in other cases a mixed profile toward several closely related isoforms of a target family is desired.^{1–3} Nevertheless, as long as highly selective tool compounds are not available, this intriguing question about the best-suited profile can hardly be answered. Therefore, the issue of sufficient drug selectivity is increasingly moving into the focus of contemporary drug research.^{4–6}

First of all, appropriate steric fit, optimal shape complementarity and high-affinity binding are usually defined as prime strategies in the development of drug molecules with sufficient selectivity. Such structural and energetic aspects of mutual protein-ligand recognition have to be accomplished to guarantee potent binding. They are established by non-covalent interactions, e.g., by forming hydrogen bonds, ionic interactions, hydrophobic contacts or van-der-Waals interactions.⁷ The resulting affinity of the formed complex is then characterized by the dissociation constant K_d which is related to thermodynamic

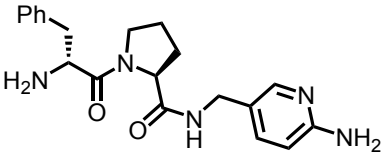
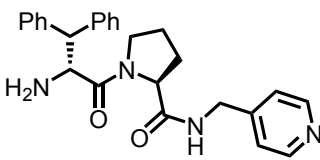
parameters such as Gibb's free energy ΔG° , binding enthalpy ΔH° and entropy $-T\Delta S^\circ$.⁸ Furthermore, before a complex assembles, both binding partners are solvated with a solvation shell of water molecules. Some of these are in loose contact with the protein or ligand, others establish strong hydrogen bonds in one or the other states. In all cases, the inventory of available degrees of freedom of the binding partners involving water molecules will change.⁹ Furthermore, water molecules can actively participate in binding and mediate contacts between protein and ligand. Changes in the solvation pattern during the entire association/dissociation process will also play an essential role in protein-ligand recognition and have an impact on affinity and particularly on binding kinetics.^{8,10,11} Thus, the sole consideration of the formed end-state complexes is usually not sufficient to explain affinity.

However, are these criteria to improve affinity toward a given isoform of a target family over another family member sufficient to achieve sufficient selectivity? Definitely, affinity enhancing features are a necessary criterion but are they also sufficient for target selectivity discrimination? Likely, more factors have to be regarded to finally achieve the desired selectivity profile. In order to equip drug molecules by rational concepts with an appropriate selectivity profile, we must first elucidate which features the proteins have at disposal to evolve their selectivity determinants.

In the present investigation, we selected the well-studied and highly similar serine proteases trypsin and thrombin for a case study. The first is an important enzyme in

1
2
3 digestion, the second displays the key enzyme in blood clotting.¹² Particularly their S1
4
5
6
7 specificity pockets, known to be most important for selectivity discrimination, are, on first
8
9
10 sight, highly similar in architecture.¹³ In literature, the only obvious residue exchange of
11
12
13 Ser190 by Ala in the pocket is made responsible for discrimination.^{14–16} On first glance,
14
15
16
17 as the Ser/Ala exchange sacrifices the option to form an additional hydrogen bond either
18
19
20
21 directly to a bound substrate or ligand molecule, or mediated via active-site water
22
23
24 molecules. This might modulate the residual solvation structure in the S1 pocket. In the
25
26
27
28 present study, we investigated the difference in binding of a congeneric series of D-Phe-
29
30
31 Pro-(amino)pyridine inhibitors with slightly deviating basic character of their C-terminal P1
32
33
34
35 residue toward thrombin and trypsin by X-ray crystallography and by isothermal titration
36
37
38 calorimetry (ITC). Both proteases recognize substrates with basic P1 residues via binding
39
40
41
42 to Asp189 at the bottom of their S1 pocket. Surprisingly, thrombin is highly selective to
43
44
45 recognize natural P1-Arg substrates whereas trypsin possesses a much broader
46
47
48
49 substrate specificity and cleaves unselectively after P1-Arg or P1-Lys residues.^{14,17,18} One
50
51
52 obvious difference between these two basic amino acids is a significant difference in their
53
54
55
56 pK_a values. Nevertheless, such values can be strongly modulated depending on the local
57
58
59
60

environment in their binding pockets. E.g. in a hydrophobic pocket, either acidic or basic ligand head groups will less likely adopt a charged state whereas a basic ligand group becomes easily positively charged by protonation, when bound to a negatively charged residue in a more polar binding site. The opposite is the case if the ligand bears an acidic group and the protein provides basic residues such as Arg or Lys in the binding pocket.⁷ Consequently, the protein environment is designed in a way to induce significant pK_a shifts of titratable groups of the bound ligand. However, is there any difference caused by the Asp189 residue in trypsin and thrombin that might take a differing effect on the observed pK_a shift of titratable groups of a bound substrate or inhibitor molecule? Since ITC can determine overall changes in the protonation inventory of a binding reaction, we studied our compound series with deviating basic character in parallel against trypsin and thrombin. Remarkably, a difference is found indicating that one ligand of the series binds to trypsin in protonated state at its basic anchor group, whereas the same ligand is accommodated in the S1 pocket of thrombin in neutral state. This experimental observation suggests that the two Asp residues in both proteases show different electrostatic properties and supposedly contribute to features of the two proteases responsible to achieve selectivity discrimination in the otherwise sterically nearly identical S1 pockets.

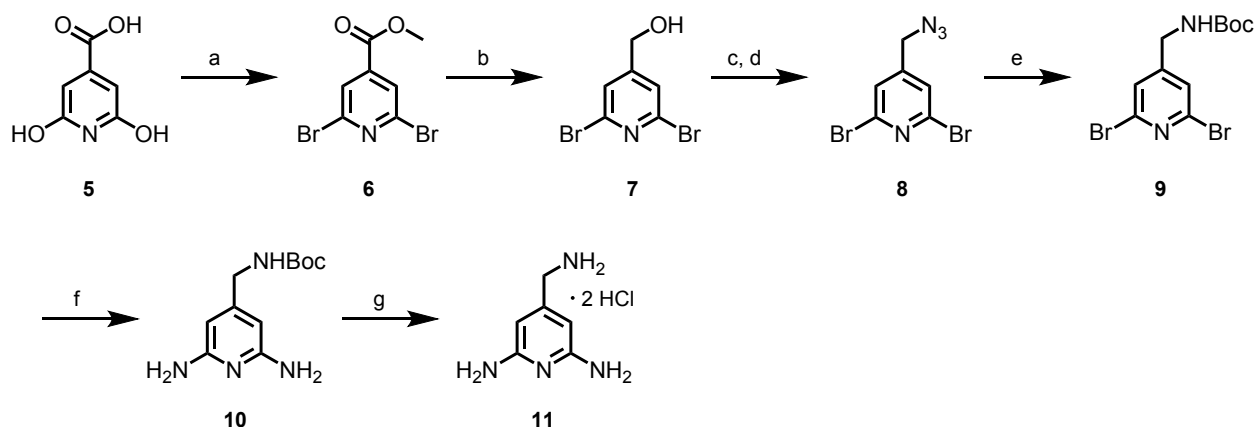
1				
2				
3				
4				
5				
6	3		140 ± 15	47 ± 7
7				6.3
8				
9				
10				
11	4		1213 ± 39	497 ± 36
12				5.0
13				
14				
15				
16				
17				
18				
19				
20				
21				
22				
23				
24				
25				
26				
27				
28				
29				
30				
31				
32				
33				
34				
35				
36				
37				
38				
39				
40				
41				
42				

^a K_i values were determined using an enzyme kinetic fluorescence assay and are given as arithmetic mean from three measurements (\pm SD). ^b pK_a values were obtained by potentiometric titration.

Synthesis. The general synthesis route for D-Phe/D-DiPhe-Pro based inhibitors was already described previously by us and other groups.^{19–22} For the present study, we focused on the same D-Phe/D-DiPhe-Pro scaffold by introducing different aminopyridines

for inhibitors **1-3** and unsubstituted pyridine for compound **4** as P1 building blocks. In the following, we will describe the synthesis of precursor **11** which was used for the amide coupling reaction with Boc-D-Phe-Pro-OH leading to the target inhibitor **1**. Inhibitors **2-4** were synthesized from commercially available precursors **12-14**. Boc-D-Phe-Pro-OH was afforded according to a protocol of Steinmetzer et al.²³, the analogously Boc-D-DiPhe-Pro-OH was obtained by adapting a similar procedure as outlined by Baum et al.¹⁹ The P1 building block **11** is a known fragment that was synthesized according to a patented procedure published by Hoffmann-La Roche Inc. in 2003. There, the synthesis was performed using gaseous reagents which were reacted under high pressure (up to 20 bar).²⁴ To avoid such drastic conditions, a synthesis of **11** was developed under milder conditions also suited on smaller scale (see Scheme 1).

Scheme 1. Synthesis of precursor **11**.



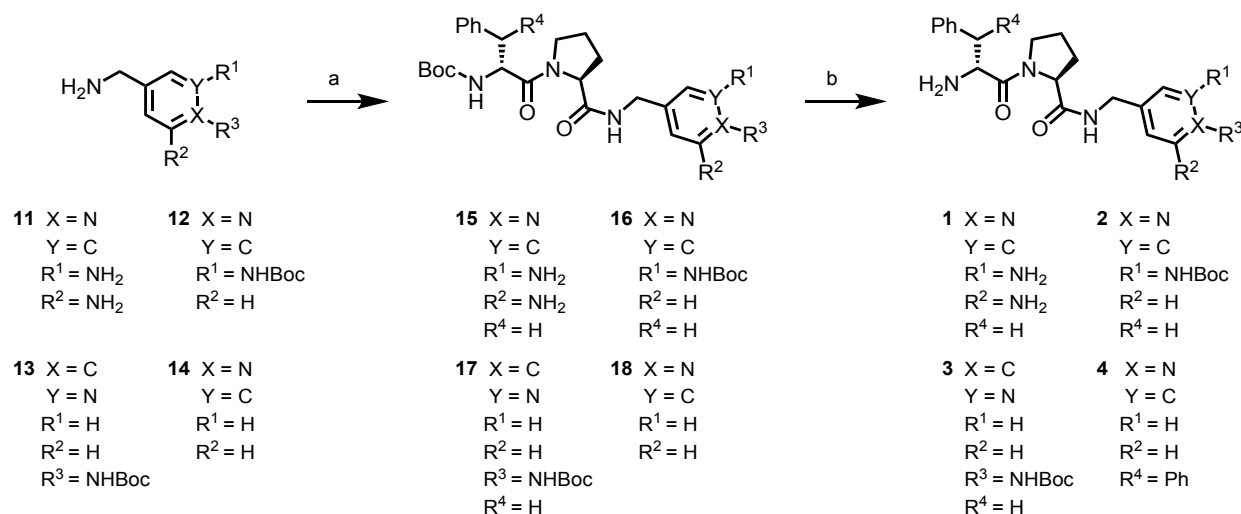
Reagents and conditions: a) POBr_3 , 130-150 °C, 2 h then MeOH, 0 °C-rt, 15 h, 74%; b) NaBH_4 , MeOH, 65 °C, 3 h, 91%; c) PBr_3 , 1,4-dioxane, 40 °C, 3 h; d) NaN_3 , DMF, rt, 24 h, 66% (over 2 steps); e) PMe_3 , THF, 0 °C-rt, 3 h then Boc_2O , NEt_3 , THF, 0 °C-rt, 3 h, 50%; f) 25% (w/v) $\text{NH}_3(\text{aq})$, Cu_2O , DMEDA, K_2CO_3 , ethylene glycol, 60 °C, 16 h, 63%; g) 4 M HCl in 1,4-dioxane, rt, 3 h, 95%.

Precursor 11 was obtained from citrazinic acid 5 which was converted into 6 via bromination and esterification.²⁵ Methyl ester 6 was reduced to the corresponding alcohol 7,²⁶ followed by bromination and azidation to 8. Compound 8 was used for a one-pot Staudinger reaction and Boc-protection to afford the Boc-amine 9.^{27,28} In the next step, the two amino groups could be introduced via an Ullmann reaction to provide intermediate 10 according to a procedure described by Elmkaddem et al.²⁹ Cleavage of the protecting group was performed under acidic conditions to yield the P1 building block 11 as double HCl salt for the subsequent synthesis of inhibitor 1. Due to the minor

nucleophilicity of the aromatic amino groups in compound **11**, the primary aliphatic amino function reacted exclusively by forming the wanted amide.

In Scheme 2 the amide coupling is described for each precursor **11-14** (**12** and **13** were commercially available from ChemPUR, **14** from Sigma Aldrich) to the respective Boc-D-Phe/D-DiPhe-Pro derivative **15-18**. In the final step, intermediates **15-18** were deprotected using TFA to the desired inhibitors **1-4** as double TFA salts.

Scheme 2. Synthesis of inhibitors **1-4**.



Reagents and conditions: a) Boc-D-Phe-Pro-OH (for **15-17**), Boc-D-DiPhe-Pro-OH (for **18**), HOBt, EDC · HCl, DMF, DIPEA, 0 °C-rt, 18-24 h, 65-78%; b) TFA, rt, 2 h, 78-92%. R³ exists only for **3**, **13** and **17**.

X-ray Crystallography. The four D-Phe/D-DiPhe-Pro-based thrombin and trypsin inhibitors were analyzed by X-ray crystallography. Eight crystal structures were obtained with a resolution of 0.95-1.57 Å.

The diaminopyridine structure of inhibitor 1 (Figure 1A) uses its polar head group to interact with Asp189 at the bottom of the S1 pocket of either thrombin or trypsin. The ortho amino groups make contacts to Gly219 and the water molecule W2 whereas the pyridine-*N* undergoes a water mediated interaction with Asp189 via W1. In case of thrombin, additional interactions are experienced by the “left” exocyclic amino group with the carboxylate group of Glu192. Furthermore, this residue adopts a back-folded conformation to participate via the interstitial water molecule W3 in the binding of the P3 group and via W4 in the formation of a contact to the P2 group. In trypsin, this contact is not found and residue 192 is here replaced by a corresponding Gln which is disordered in this structure (Figure 1E). Due to the exchange of Ala190 to Ser in the trypsin complex, the Ser190 sidechain interacts directly with water molecule W2 and the “right” amino group. This amino group performs additionally an interaction to the backbone carbonyl group of Ser190 and to the carboxylate group of Asp189. Structurally, the back-folding of

Glu192 in thrombin to undergo a water-mediated contact to **1** seems to be replaced in trypsin by the unique Ser190O γ H-bond to the ligand, which is further supported by a contact to the more firmly fixed water molecule W2 in the latter protease.

The P1 residue of inhibitor **2** is bound in two conformations (Figure 1B, 76% for I and 24% for II) in the S1 pocket of thrombin. Thus, it formally mimics the binding mode of **1**. In orientation I, the amino group is orientated toward Tyr228 by forming a hydrogen bond with the water molecule W2, in the other orientation, its amino group points in the direction of Gly219 while the pyridine-*N* interacts with Asp189 via water molecule W1 in both conformations. A related binding mode can be assigned to the trypsin structure (Figure 1F), however, here ligand **2** adopts only one conformation by addressing W2 and Ser190O γ on the “right” side via its amino group, and it is involved in an additional direct H-bond to the carboxylate of Asp189. A very similar interaction pattern is found for **1** and **2** toward Tyr228 as observed in thrombin forming water-mediated interactions of the amino group or the pyridine-type *N* to the carboxylic function of Asp189 and the water molecule W2 hosted on top of the phenyl moiety of Tyr228. Also in the thrombin-inhibitor complex with **2**, the residue Glu192 is in a back-folded conformation to interact via water

molecule W3 to the P3 group and via W4 to the P2 group. In trypsin such contacts are missing and the corresponding Gln192 does not adopt a folded geometry to allow contacting the P1 ligand head group. Possibly, the charged Glu192 in thrombin is responsible for the observed dual orientation of the head group, even so the conformer hydrogen-bonding this residue is the lower populated one. Analogously to the trypsin complex of **1**, Ser190 is able to form the same interactions to W2 and the amino group of the ligand, which is furthermore in both proteases in contact to Asp189 and the backbone carbonyl group of then residue in position 190.

Inhibitor **3** is a regio-isomeric aminopyridine derivative of compound **2**, in which the P1 moiety is para-substituted by the amino group while the pyridine-*N* is in meta position with respect to the D-Phe-Pro scaffold. The thrombin complex (Figure 1C) indicates a direct hydrogen bond to Asp189 complemented by further interactions to the backbone carbonyl oxygens of Ala190 and Gly219, while the pyridine-*N* interacts with W2. Glu192 establishes the same interaction geometry as found for the complexes with inhibitor **1** and **2** by water-mediated contacts to the P2 and P3 moiety via W3 and W4. For the P1 group, a similar binding pose can also be observed in the trypsin complex (Figure 1G) in which

1
2
3
4 either direct or water-mediated (W1) interactions are formed to both oxygens of the
5
6
7 carboxylate of Asp189. Furthermore, in the trypsin complex with inhibitor **3**, the Ser190
8
9
10 sidechain interacts directly with the pyridine-*N*. Due to this direct contact to Ser190, W2
11
12
13 is shifted to the rear of the pocket but still interacts with the pyridine-*N* and with the
14
15
16 hydroxy group of Ser190. The sidechain of Gln192 is disordered and not visible in the
17
18
19 trypsin complex with ligand **3**. Surprisingly, there is a second conformation observed for
20
21
22 the aromatic ring of the terminal phenylalanine attached at the P3 position, which,
23
24
25 however, has no influence on the binding mode of the P1 group.
26
27
28
29
30

31 The refined interactions of inhibitor **4** are comparable in both cases and do not suggest
32
33
34 any structural differences in the S1 pocket among the complexes with the two enzymes.
35
36
37
38 Figure 1D shows the binding mode of inhibitor **4** in thrombin. This ligand is the analog of
39
40
41 a compound studied in a previous contribution by us that possesses a D-diphenylalanine
42
43
44 as P3 group, but with respect to P1 and P2 it describes the same binding mode as the D-
45
46
47 monophenylalanine derivative.²¹ As reported earlier, the unsubstituted pyridine ring of the
48
49
50 P1 head group forms an indirect interaction with Asp189 mediated by two water
51
52
53 molecules (W1 and W5). They are found at sites, which are not fully occupied (each with
54
55
56
57
58
59
60

50% occupancy) and show a close mutual distance of 2.0 Å along with reasonable *B*-factors (23-24 Å²). An additional water molecule (W6) is found at a site, which was set to 50% occupancy with a distance of 2.1 Å to W1 and an acceptable *B*-factor (23 Å²). A similar disordered water pattern between the pyridine-type nitrogen and Asp189 has been described in our previously determined structure of the D-Phe-Pro analog with thrombin.²¹ Remarkably, we observed for **4** a very similar binding mode as for the aminopyridine inhibitors **1** and **2**, however in all analogous trypsin complexes the pyridine-*N* interacts with Asp189 via a single and fully occupied water molecule found in one distinct spatial position. Residue Ser190 indicates two conformations which are possibly only resolved in this complex due to the achieved high resolution of 0.95 Å. Conformation I (occupancy of 79%) orientates to water molecule W2 while the other (II, occupancy of 21%) is in contact with the sidechain of Tyr228. We can therefore summarize that the major difference between the thrombin and trypsin complexes with **4** are the following: In thrombin, the contacts between **4** and Asp189 are formed via a network of hydrogen-bonds, however refinement suggests that water is here distributed over several hydration

1
2
3
4
5
6
7
8
9
10
11
12
13
14
15
16
17
18
19
20
21
22
23
24
25
26
27
28
29
30
31
32
33
34
35
36
37
38
39
40
41
42
43
44
45
46
47
48
49
50
51
52
53
54
55
56
57
58
59
60

sites whereas in trypsin the carboxylate of Asp189 reinforces an ordered contact mediated by a single water molecule.

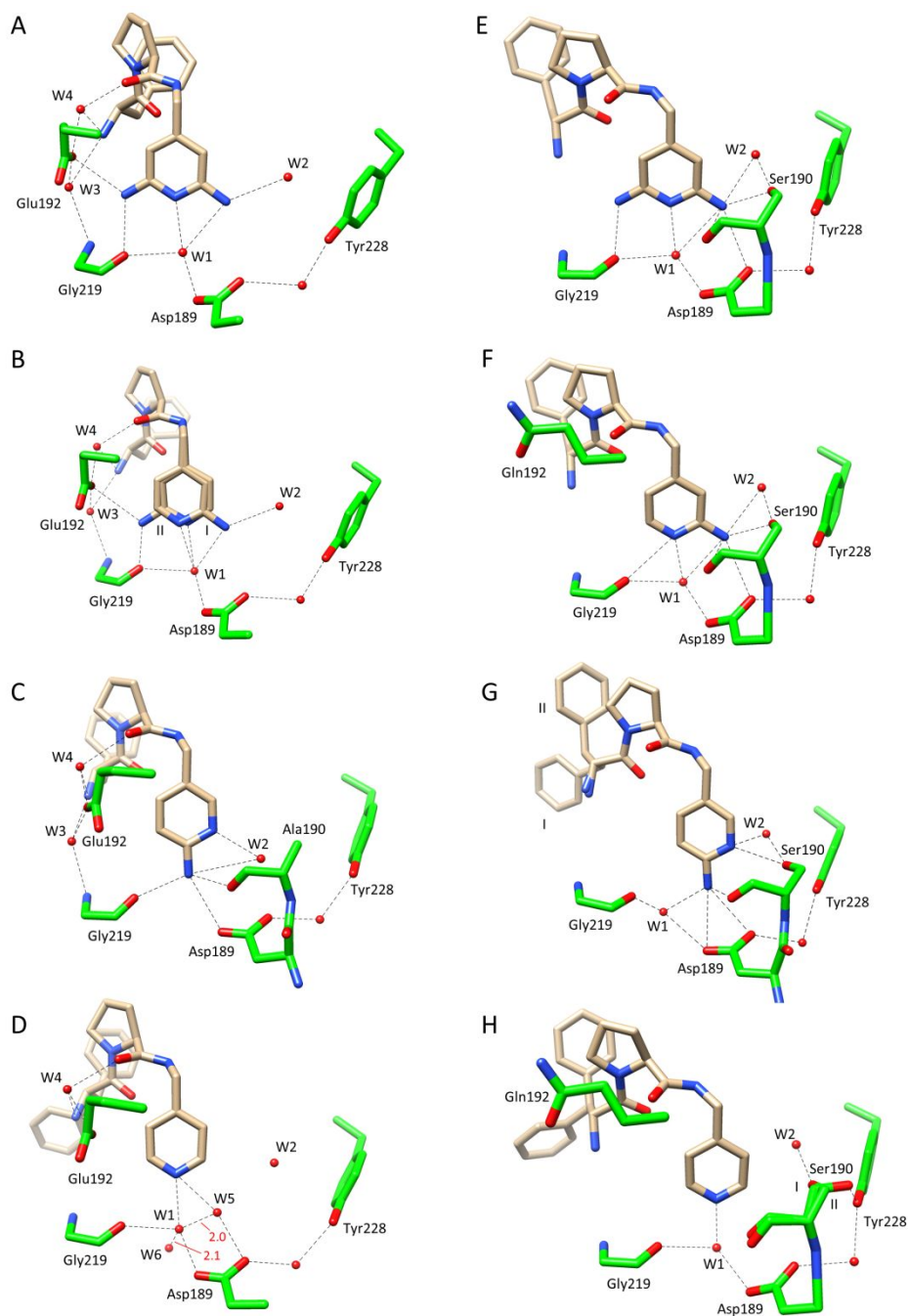


Figure 1. Binding modes of inhibitors 6HSX (1, A), 6T3Q (2, B), 6T4A (3, C) and 6TDT (4, D) in the S1 pocket of thrombin (left) compared to the structures of trypsin (right) by inhibitors 6T0M (1, E), 6T0P (2, F), 6T5W (3, G) and 6SY3 (4, H). The inhibitors are represented in light brown whereas the protein residues are displayed in green. Heteroatoms are color-coded by atom type. Water molecules are colored in red and favorable hydrogen bonds are shown as dashed lines.

The distances in the complex of thrombin between the water molecules (W1, W5, W6) at the bottom of the S1 site are given in Å and are colored in red. In the trypsin complexes with **1** (E) and **3** (G), Gln192 is not visible due to the weakly defined mF_o-DF_c electron density of this residue after refinement. Likely it is scattered over multiple orientations.

ITC Data Collection. For all inhibitors of the series, we can assume that the polar head groups become at least partly protonated at the pyridine-*N* upon binding to the S1 pocket. This is in agreement with our previous studies, which suggested significant pK_a shifts of the basic anchor groups once bound next to the charged protein residues.³⁰ Accordingly, we studied the entire series by ITC titrations in different buffers to record putatively overlaid changes in protonation states. The values obtained for the different buffers are listed in Table 2.

Table 2. Thermodynamic data of ΔH° from direct ITC titrations in thrombin and trypsin.

Inhibitor	Thrombin				Trypsin		
	$\Delta H^\circ /$	$\Delta H^\circ /$	$\Delta H^\circ /$	$\Delta H^\circ /$	$\Delta H^\circ /$	$\Delta H^\circ /$	$\Delta H^\circ /$
	kJ mol ⁻¹	kJ mol ⁻¹	kJ mol ⁻¹	kJ mol ⁻¹	kJ mol ⁻¹	kJ mol ⁻¹	kJ mol ⁻¹
	Phosphate	HEPES	Tricine	Tris	HEPES	Tricine	Tris
1	-107.0 ± 1.0	-87.5 ± 0.7	-80.6 ± 0.8	-64.7 ± 1.1	-39.1 ± 1.7	-30.5 ± 0.3	-17.7 ± 0.5

2	-83.7 ± 0.5	-64.9 ± 0.1	-54.5 ± 0.5	-42.3 ± 0.2	-36.9 ± 0.9	-27.2 ± 1.8	-13.0 ± 1.0
3	-97.6 ± 0.3	-76.7 ± 0.4	-32.0 ± 0.7	-22.9 ± 0.9	-36.8 ± 0.5	-29.5 ± 0.2	-16.4 ± 1.0
4	-30.8 ± 1.1	-26.8 ± 1.3	-24.8 ± 0.5	-24.3 ± 0.9	-	-	-
4^a	-23.2 ± 1.2	-	-	-27.1 ± 0.6	-35.7 ± 1.9	-18.5 ± 0.3	-1.0 ± 1.0

Standard deviations were determined from triplicate measurements. $^a\Delta H^\circ$ is given as the observed enthalpy by a control experiment using **19** as a displacement ligand (Table S2) which confirm the buffer independence of inhibitor **4** in thrombin. For **4** both direct titration and displacement titration (**4^a**) are listed. The displacement titration was performed in phosphate and Tris buffer since their ionization enthalpies have the largest difference of the chosen buffers.^{31,32} Due to the low binding affinity of **4** in trypsin, the values of **4** were obtained by displacement titration.

As a pronounced buffer dependence has been observed, we can definitely conclude that changes in protonation state are given for the individual ligands (s. Figure 2 and discussion below). To relate the observed quantities to well-defined reference values in aqueous solution, we determined the pK_a properties of our four ligands experimentally in aqueous solution (Table 3). As suggested by the crystal structures and the order/disorder phenomena observed next to Asp189, the unsubstituted derivative **4** indicates different

binding properties in thrombin and trypsin. We therefore investigated particularly this ligand in more detail by ITC experiments (s. below).

Table 3. Protonation Effects of Inhibitors 1-4 in Thrombin and Trypsin.

Inhibitor a	Δn_{H^+} (Thrombin)	Δn_{H^+} (Trypsin)	pK_a1^b	pK_a2^b
1	0.94	0.81	6.4	7.5
2	0.95	0.90	6.7	7.5
3	0.87	0.78	6.3	7.5
4	0.15	1.30	5.0	6.6

^aThe protonation state of all four inhibitors were determined by direct titrations except of **4** in trypsin. The latter measurement was performed by a displacement titration. ^bThe pK_a values were determined by potentiometric titration and describe the acidity of the P1 head group (pK_a1) and the N-terminal amino group (pK_a2) in protonated state.

Protonation effects recorded by ITC. Table 3 lists the overall changes of the protonation inventory of the respective inhibitors which describes the exchange of protons (Δn_{H^+}) during the binding reaction between ligand, protein and buffer. The measured heat signals were plotted against the heat-of-ionization of the respective buffer and a linear correlation

is indicated. The slope of the linear fit (Figure 2) gives the molar amount of protons transferred during the entire binding process. It can be concluded that the aminopyridine derivatives **1**, **2** and **3** receive between 0.78 to 0.94 moles of protons upon accommodation to the S1 pocket of both proteins.

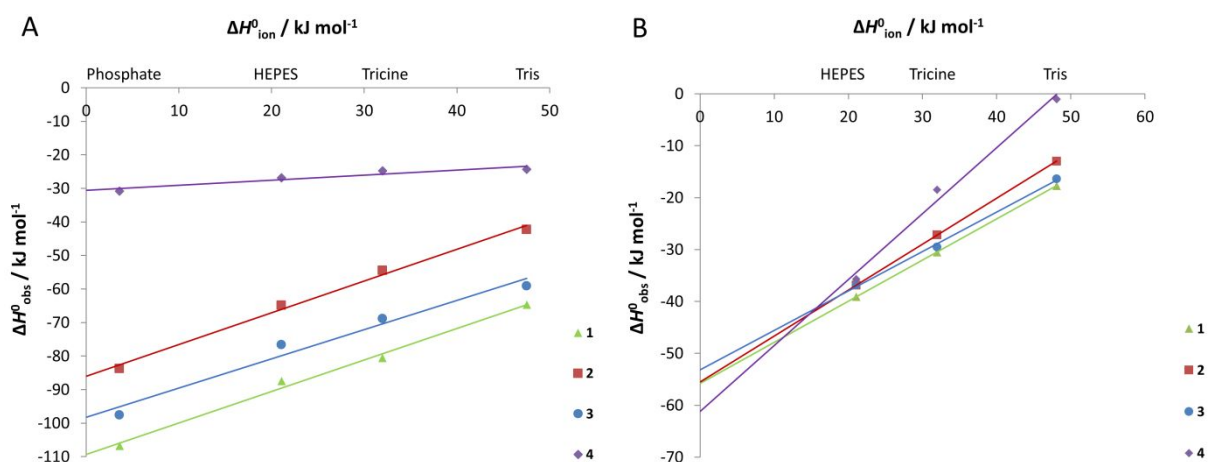


Figure 2. The diagrams (A: thrombin, B: trypsin) display the experimentally determined enthalpies $\Delta H^{\circ}_{\text{obs}}$ of the inhibitors **1-4** under different buffer conditions. They are plotted against the heat-of-ionization $\Delta H^{\circ}_{\text{ion}}$ (Phosphate³²: 3.60 kJ mol⁻¹, HEPES³¹: 21.01 kJ mol⁻¹, Tricine³¹: 31.97 kJ mol⁻¹, Tris³²: 47.53 kJ mol⁻¹) of the respective buffers. The slopes of the linear fit give the molar amounts of protons that are transferred between buffer, protein and ligand upon binding (Table 3). The intercept of these plots is reported as 'buffer corrected' value (Figure 3, Table 4).

We studied the protonation inventory of this type of inhibitors already in detail in previous contributions.^{19,21,33–38} The investigated D-Phe-Pro derivatives contained a P1

benzamidino group, which is permanently charged both in the buffer and in the protein-bound state. Additionally, the *N*-terminal group is partially charged in the buffer and reveals full protonation in the complex. Furthermore, in all complexes His57 releases 0.50-0.60 moles of protons upon ligand accommodation.³³ Thus, overall, the proton release from His57 and the entrapment by the ligand's terminal P3 amino group is virtually compensated, leaving no net protonation effect for this type of ligands.^{34,35} We assume, the same inventory applies for the latter groups in **1-4**.

However, as a difference to the permanently charged P1-benzamidino derivatives, we studied here the weakly basic (amino)pyridine derivatives **1-4** and their P1 moieties possess pK_a values of 5.0-6.7 in aqueous solution. According to the Henderson-Hasselbalch equation, all four inhibitors **1-4** will be largely deprotonated under the applied buffer conditions at pH 7.8 prior to protein binding (maximally ~ 5-10% may be protonated in the buffer). Based on the results listed in Table 3, we assume the ligands experience a pK_a shift upon binding, reinforced by the spatial neighborhood to the negatively charged Asp189 residue. This leads to full protonation of the pyridine-*N* in **1-3** for both, trypsin and thrombin. Obviously, ligand **4** behaves differently and shows protonation only in trypsin

(Table 3, Figure 2). Schiebel et al. could prove full protonation of aniline in trypsin, despite of its rather low pK_a of 4.0, by a neutron diffraction study.³⁰ Obviously, Asp189 has such a strong influence on the protonation state of the bound ligand and probably polarizes its neighborhood so strongly that a pK_a shift of several orders of magnitude is induced, triggering full protonation of the ligand, even in case of a weakly basic aniline or pyridine residue.³⁰ For this reason, we conclude that the inhibitors **1-3** entrap 0.78-0.95 moles of protons upon binding in both serine proteases besides the mutual compensation effect of the terminal amino function ($pK_a = 7.5$ for **1-3**,) which also becomes fully protonated upon binding along with the release of 0.5-0.6 moles of protons from His57.

Surprisingly, binding of inhibitor **4** reveals a deviating protonation inventory for both enzymes. Even though both complexes show almost identical binding poses in the S1 pocket, the unsubstituted pyridine derivative **4** binds, as expected, in protonated state at its pyridine-*N* to trypsin. Since the pyridine-*N* in **4** ($pK_a = 5.0$) is less basic than the head groups of **1-3** ($pK_a = 6.3-6.7$), a slightly larger molar amount of protons must be entrapped. As mentioned above, we decided to study the ligand with a second phenyl group at P3 to increase the binding affinity toward the enzymes. By this, also the pK_a

value of the *N*-terminal amino group is slightly shifted compared to **1-3**. This may also give rise to a slightly altered protonation inventory. Finally, due to lower affinity, the protonation effect of **4** during binding to trypsin could not be determined by direct ITC titration. Instead, we had to apply displacement titrations for **4** in three different buffers to trace the changes in protonation state. Possibly, the displacement titrations increase the estimated inaccuracy of this experiment due to error propagation. Nevertheless, the recorded value of 1.30 moles of protons clearly indicates full protonation of the pyridine-*N*head group of **4** in trypsin.

Unexpectedly, **4** shows a different protonation effect upon binding to thrombin, as no entrapment of a proton was registered at the pyridine-*N*head group. In a former study by Biela et al.²¹, we could investigate the analogous D-Phe-Pro ligand and it showed no obvious structural influence on the binding pose in the S1 pocket, thus we believe that the binding mode and protonation inventory of the D-Phe-Pro analog and **4** can be directly compared to the aminopyridine derivatives **1-3**. Overall, only 0.15 moles of protons are transferred upon binding of **4** to thrombin (note that a minor difference can result from the slightly shifted pK_a value observed for the D-DiPhe derivative), an amount which, as it falls

close to the experimental accuracy, speaks for no protonation of **4** at the pyridine-*N* head group in the complex with thrombin. This observation agrees with the data of Biela et al., who also did not observe any protonation of the P1 pyridine head group at their D-Phe-Pro analog. However, they had to study the protonation inventory by displacement titration. Similarly to a protocol by Biela et al.²¹, we titrated the strong binding ligand **19** to displace **4** (Table S2) as a control experiment and also by this displacement protocol no change in the protonation state could be observed ($\Delta n_{\text{H}^+} = -0.09$ mol).

Table 4. Thermodynamic data of ΔH° , ΔG° ^a and $-T\Delta S^\circ$ ^b from direct ITC titrations in thrombin and trypsin.

	Thrombin	Trypsin
--	----------	---------

Inhibitor	ΔH° / kJ mol ⁻¹	ΔG° / kJ mol ⁻¹	$-T\Delta S^\circ$ / kJ mol ⁻¹	K_d / nM	ΔH° / kJ mol ⁻¹	ΔG° / kJ mol ⁻¹	$-T\Delta S^\circ$ / kJ mol ⁻¹	K_d / μ M
1	-109.4	-39.8	69.6	100	-56.2	-23.8	32.4	68
2	-86.0	-34.4	51.6	916	-56.1	-25.3	30.8	38
3	-98.2	-36.5	61.7	400	-53.6	-24.9	28.7	43
4	-30.6	-29.4	1.2	3681	-61.9 ^c	-17.7 ^c	44.3 ^c	757 ^c

All results are presented as buffer-corrected values. ^a ΔG° is given as the mean over the results by titrations in different buffers (Phosphate, HEPES, Tricine and TRIS; in case of trypsin without phosphate). ^b $-T\Delta S^\circ$ has been calculated as the difference between ΔG° and the buffer corrected ΔH° values. ^cThese values were obtained by displacement titrations.

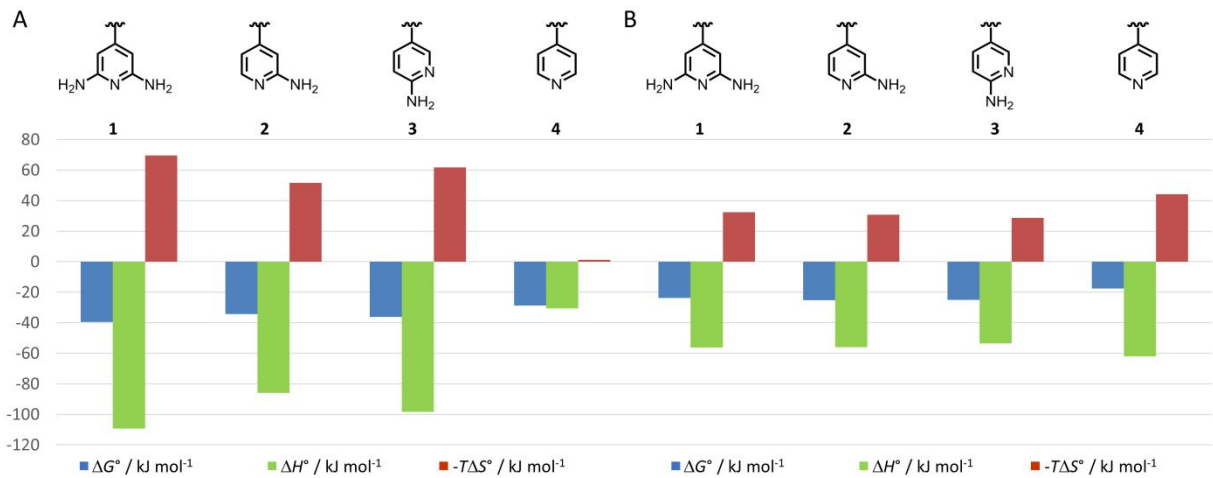


Figure 3. Thermodynamic signatures of the inhibitors 1-4 in complex with thrombin (A) and trypsin (B). The results are represented as buffer-corrected values listed in Table 4. They were determined by direct titration in thrombin. Notably, due to the relatively weak affinity of the studied ligands toward trypsin (K_i values between 40-500 μ M) all ITC measurements with trypsin have been performed as displacement titrations.

Comparison of the thermodynamic signatures. In the following, the buffer corrected values, which result from a linear extrapolation to hypothetical buffer conditions with zero heat-of-ionization (Figure 3 and Table 4) will be discussed. Based on the ITC data, we computed K_d values and they match within 3x standard deviation with the K_i values from our enzyme kinetic assay (Table 1 and Table 4). Apart from the fact that very different signals are evaluated to obtain the inhibitory potency, the meaning of K_d as ITC dissociation constant and K_i as inhibitory constant from an enzyme assay are not identical.

The three aminopyridine inhibitors **1-3** show similar signatures in their thermodynamic profiles toward thrombin. The Gibb's free energy ΔG° of all ligands falls into a range of -34 to -40 kJ mol⁻¹ resulting from an enthalpically more favored binding profile. This can be explained by the charge-assisted interactions to Asp189, sometimes mediated by interstitial water molecules. Further interactions are formed by the amino groups of **1** with Gly219 and Glu192. Furthermore, contacts with the water molecules W1 and W2 are found. In summary, these interactions give rise to a very strong enthalpic signature (ΔH°

= -109.4 kJ mol⁻¹) of **1**, closely followed by the other aminopyridine derivatives ($\Delta H^\circ = -86.0$ kJ mol⁻¹ for **2** and $\Delta H^\circ = -98.2$ kJ mol⁻¹ for **3**), which exhibit only a single amino group for interactions. The ligands are the most enthalpic binders found so far with this scaffold.^{20,21,36–38} The stronger enthalpic signature compared to the analogous benzamidine derivative results from the enthalpically less-expensive desolvation of the P1 head groups in **1–3** which are uncharged in solution prior to protein binding and only become charged in the binding pocket. This is definitely a desirable scenario, as enthalpically binding ligands have been favored as development candidates³⁹ and the mere change of the protonation state at the protein binding site helps to design molecules with improved bioavailability as charged species exhibit unfavorable PK properties. The large enthalpic signature is compensated by an unfavorable entropic contribution. Ligands **1** and **3** are separated by a $-T\Delta\Delta S^\circ_{3\rightarrow1}$ difference of -7.9 kJ mol⁻¹, whereas **2** differs even more in entropy ($-T\Delta\Delta S^\circ_{2\rightarrow1} = -18.0$ kJ mol⁻¹ and $-T\Delta\Delta S^\circ_{2\rightarrow3} = -10.1$ kJ mol⁻¹). Its slightly increased entropic advantage over **1** and **3** results from the fact that **2** is able to bind with two alternative conformations (Figure 1B), which is, with respect to the inventory of degrees of freedom, entropically beneficial.

The unsubstituted pyridine derivative **4** shows weaker thrombin binding and, to enable direct ITC titrations at least with thrombin, we selected the analogous diphenyl derivative with a by a factor of 10 enhanced affinity (Baum et al.²⁰). Overall, **4** binds with reduced enthalpic signature, likely as it does not exhibit a P1 group that establishes a charge-assisted contact with Asp189. Instead, the carboxylate group is connected via a network of disordered water molecules which likely also contributes to an entropically more favored binding signature (Figure 1D, Figure 3A).

If we compare the thrombin results with those for trypsin of the same ligands, it is remarkable to see by how much the binding affinity decreases for **1** ($\Delta\Delta G^{\circ}_{\text{thrombin} \rightarrow \text{trypsin}} = -16.0 \text{ kJ mol}^{-1}$), **2** ($\Delta\Delta G^{\circ}_{\text{thrombin} \rightarrow \text{trypsin}} = -9.1 \text{ kJ mol}^{-1}$) or **3** ($\Delta\Delta G^{\circ}_{\text{thrombin} \rightarrow \text{trypsin}} = -11.6 \text{ kJ mol}^{-1}$) although very similar interactions are established in trypsin's S1 pocket (Figure 1E-H).

The reduced binding affinities toward trypsin in the two-digit micromolar range made displacement titrations necessary in these cases (Table 1).^{40,41} Since the S1 pockets are very similar for both proteins, the S2 and S3/4 pockets play an important role to gain affinity. Thrombin is able to form strong hydrophobic contacts with the P2 proline moiety via its 60's-loop while the P3 group is well conserved in the S3/4 pocket also by

hydrophobic interactions.⁴² Additionally, the thrombin complexes show that Glu192 adopts a back-folded geometry stabilizing the amide groups of the D-Phe-Pro scaffold and establishing polar contacts to the P1 head group (Figure 1A-D). In trypsin, Glu192 is replaced by Gln, which cannot form a charge-assisted contact. This all contributes to an enthalpic signature, which is not similarly possible in case of trypsin. Consequently, affinity drops in the trypsin case compared to thrombin. Due to the stronger directional interactions with thrombin, the ligands most likely also entail a loss of degrees of freedom as they become more firmly fixed compared to the trypsin complexes. This explains to some extent the entropically more beneficial binding signature of **1-3** to trypsin. Facing the trypsin and thrombin data for ligand **4** shows different behavior, as it binds to the former protease with a charged head group, thus improving the enthalpic binding contribution. Furthermore, since a network of disordered water found in thrombin to mediate the contact to Asp189 becomes ordered in trypsin, the binding of **4** to trypsin becomes entropically less favored. Overall however, as the affinity enhancing effects contributed by the interactions experienced in the S2 and S3/4 pockets of both proteases are quite different, a mutual comparison of the binding and thus selectivity features of

1
2
3 the four ligands toward thrombin and trypsin is difficult. Nevertheless, main purpose of
4
5
6
7 this study was to trace the selectivity determinants provided by trypsin and thrombin in
8
9
10 their S1 pockets.
11

12
13 **Different charge density of Asp189 influences the protonation effect.** We already
14
15
16
17 observed in our previous neutron diffraction study on trypsin that Asp189 can induce
18
19
20
21 strong pK_a shifts of the adjacent ligand functional groups once bound to the S1 pocket.³⁰
22
23
24 Compounds **1-3** experience a change in protonation either in thrombin or in trypsin
25
26
27 leading to a charge-assisted interaction partly mediated via W1 (Figure 1A-C, 1E-G). In
28
29
30
31 addition, the change of the protonation state will be stabilized by mesomeric effects
32
33
34 assisted by the adjacent amino groups to delocalize the positive charge. The ITC results
35
36
37
38 recorded for **4** show that this ligand binds unprotonated to thrombin but protonated to
39
40
41
42 trypsin. This difference is also reflected by the local network of disordered vs. ordered
43
44
45 water molecules formed between the P1 head group and Asp189. We believe the local
46
47
48 environment of Asp189 and the involved charge distribution provides an explanation for
49
50
51
52 these differences. In total, three differences are observed between the S1 pockets of
53
54
55
56 trypsin and thrombin. First of all, a Ser190Ala replacement is given, which however, has
57
58
59
60

no obvious impact on the binding poses in the current cases. Secondly, the Gln192Glu replacement adds another charged residue in case of thrombin, which fairly adaptively, adopts in the studied complexes a back-folded geometry bringing its likely charged carboxylate group in the neighborhood of the P1 head group. Finally, the main difference between the two serine proteases is the presence of a sodium ion in thrombin which is about 5.3 Å remote from Asp189. It shows octahedral coordination geometry formed by four water molecules and the backbone of carbonyl groups of Arg221A and Lys224 (Figure 4). In general, Na⁺ is responsible for regulating the protein activity^{43,44} as the Na⁺-bound form cleaves procoagulant substrates at faster rates, whereas the Na⁺-free form is less efficient and called the 'slow form'.⁴⁵ With respect to our studied ligand series, we assume that the presence of this cation has an electrostatic influence on the charge distribution on Asp189 and might attenuate its negative charge. Due to a reduced charge localization on the carboxylate oxygens of this residue, the interaction with the adjacent ligand functional groups is weakened. Supposedly, for the less basic pyridine moiety of **4** the polarization effect is no longer sufficient to reinforce protonation of the pyridine-*N* in case of thrombin. In the trypsin complex, where no comparable Na⁺ is located next to

Asp189, the charge attenuation of Asp189 is not in operation so that the highly negatively charged carboxylic group exerts stronger polarization effects, apparently still sufficient to induce a protonation of the ligand's head group. Simultaneously, it establishes a well-ordered water-mediated charge-charge interaction with the ligand. This hypothesis has already been proposed in our previous study where we speculated about a different charge distribution on Asp189 between thrombin and trypsin.⁴⁶ The hypothesis was based on the deviating geometries found for *N*-amidinopiperidine in the S1 pocket of both proteases. It is found with planar geometry at the *ipso* nitrogen in thrombin whereas planar and pyramidal hybridization states were observed side-by-side in trypsin. Also here, this effect was related to a putative charge attenuation of Asp189 in thrombin.⁴⁶ Transferred to the present study, in thrombin the adjacent pyridine nitrogen of **4** remains uncharged and the fixation of the interstitial solvation shell is relaxed resulting in a network with water molecules scattered over several hydration sites. It remains speculative whether the proposed attenuated charge on Asp189 in thrombin takes also influence on the well-known substrate discrimination, as thrombin only recognizes peptide chains with the more basic P1-Arg whereas trypsin accepts in addition to P1-Arg also the less basic P1-Lys at

this position. Possibly, the charge attenuation on the carboxylate oxygens of Asp189 in thrombin results in weaker charge-assisted hydrogen bonds to the terminal amino anchor of a Lys compared to the slightly longer and deeper penetrating Arg head group which usually establishes two parallel H-bonds using its guanidinium nitrogens.

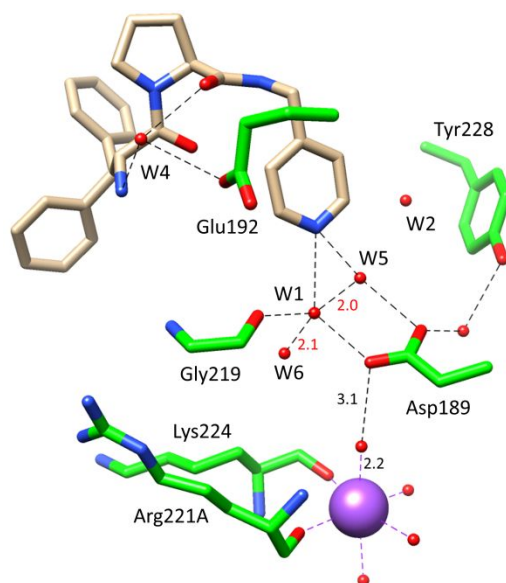


Figure 4. Binding mode of ligand 4 in the S1 pocket of thrombin (pdb-code: 6TDT) in presence of Na⁺ (purple ball) closely adjacent to Asp189. The octahedral coordination of Na⁺ is represented as dashed lines in purple. The ligand is shown in light brown whereas the protein residues are displayed in green. Heteroatoms are color-coded by atom type. Water molecules are displayed as red spheres and favorable hydrogen bonds are indicated as dashed lines with the corresponding distances in Å.

CONCLUSIONS

In this comparative study between thrombin and trypsin, selectivity discriminating features, particularly in the S1 pocket between both proteins were investigated by enzyme kinetics, thermodynamics and crystallography using a small series of D-Phe/D-DiPhe-Pro derivatives with deviating (amino)pyridine head groups. Thrombin and trypsin are structurally related proteins and possess closely similar S1 pockets which are responsible for the substrate specificity.¹⁴ Crystal structure analyses show that all four ligands adopt nearly identical binding modes in both proteins. Differences are presented by the enzyme kinetic and thermodynamic data. While the inhibitors are mainly nanomolar binders in thrombin, the binding affinity is reduced by at least two orders of magnitudes in trypsin (Table 1). We relate these differences to contacts formed in the S2 and S3/4 pockets of the proteases. The reduced binding affinity towards trypsin is also noticeable in the thermodynamic profiles. ITC experiments show that the ligands have a much stronger enthalpic contribution to binding in case of thrombin than trypsin. As a matter of fact, this effect is entropically largely compensated so that the free Gibb's energy differs by only about two orders of magnitude in K_D . By investigating putatively overlaid protonation effects, it can be seen that the slightly more basic aminopyridine derivatives ($pK_a = 6.3-6.7$) all become fully protonated in both enzymes at the pyridine-*N*, whereas protonation in the buffered solution at pH 7.8 prior to binding is hardly experienced. In addition, His57 of the catalytic triad releases about 0.50-0.60 moles of protons, which in turn, is compensated by the terminal amino group. It virtually entraps the same amount of protons upon protein binding. Thus, the proton exchange is compensated and the overall observed protonation effect is generated nearly exclusively by the protonation of the P1 moiety. In nearly all examples, the weakly basic P1 head groups become fully protonated in the S1 pocket as they possess pK_a values of 6.3-6.7. The observed pK_a shift is determined by the polarization of

the negatively charged Asp189 which triggers a pK_a shift in the S1 pocket and thus induces protonation at the pyridine-*N*. An astonishing difference is found for the complexes of **4** with both proteases (Figure 1D and 1H). The basicity of the pyridine derivative **4** is with $pK_a = 5.0$ about 1.5 units lower than those of **1-3**. Surprisingly, **4** remains unprotonated in case of thrombin but it entraps a proton upon binding to trypsin. We suggest to explain this difference by the presence of a sodium ion in thrombin about 5.3 Å remote from Asp189 (Figure 4). Likely, this cation has an electrostatic influence on the charge distribution on Asp189. We suppose that Na^+ attenuates the negative charge on Asp189 and thus modulates the binding properties in the S1 pocket. In consequence, the carboxylate group cannot sufficiently polarize the pyridine-*N* of **4** to induce protonation. Because of the attenuated negative charge on the carboxylate oxygens, the water-mediated charge-charge interactions between the P1 head group of **4** and Asp189 is insufficient to induce protonation at the pyridine-*N*. Contrarily, in trypsin, where Na^+ is absent the polarizing effect is strong enough to succeed in full protonation of the pyridine-type head group.

EXPERIMENTAL SECTION

Enzyme Kinetic Fluorescence Assay. The inhibition of human α -thrombin (Beriplast®, CSL Behring, Marburg, Germany) was investigated by a fluorescence assay using Tos-Gly-Pro-Arg-AMC · TFA as fluorogenic substrate in black 96-well plates with a Fluoroskan Ascent fluorometer (Thermo Fisher Scientific, Vantaa, Finland; $\lambda_{ex} = 380$ nm, $\lambda_{em} = 460$ nm) according to Stürzebecher et al.⁴⁷ The measurements were performed at 25 °C

1
2
3 in a buffer composed of 50 mM Tris, 154 mM NaCl, 0.01% (w/v) PEG8000 at pH 7.8. The
4
5
6
7 final thrombin concentration was 80 pM while the inhibitors were dissolved in DMSO and
8
9
10 diluted in buffer to reach a final DMSO concentration below 1% (v/v) in the assay. For the
11
12
13 determination of the inhibition constant K_i , substrate concentrations of 2.5, 5.0 and 10 μ M
14
15
16
17 were used at four different inhibitor concentrations together with control measurement in
18
19
20 absence of inhibitor in a total volume of 140 μ L. Analogically, the inhibition of bovine
21
22
23 trypsin (Sigma Aldrich, product number T8003) was performed with Mes-D-Arg-Gly-Arg-
24
25
26
27 AMC · 2 TFA as fluorogenic substrate at a protein concentration of 65 pM. Here,
28
29
30
31 substrate concentrations of 6.3, 12.5 and 25 μ M were used. The buffer contained 43 mM
32
33
34 Tris, 132 mM NaCl, 0.0086% (w/v) PEG8000 at pH 7.8.
35
36
37

38 The velocities were obtained from the slopes of the progress curves during a time frame
39
40
41 of 5 min and all K_i values were determined by a non-linear fit to the Michaelis-Menten
42
43
44 equation. All measurements were performed at least in triplicate.
45
46
47

48 **Synthesis.** ^1H and ^{13}C NMR spectra were measured on a JEOL ECX-400 or JEOL ECA-
49
50
51 500 instrument. Chemical shifts are reported in ppm using residual peaks for the
52
53
54 deuterated solvents as internal standard:⁴⁸ 7.26 ppm (^1H NMR), 77.2 ppm (^{13}C NMR),
55
56
57
58
59
60

CDCl₃; 2.50 ppm (¹H NMR), 39.5 ppm (¹³C NMR), DMSO-*d*₆. The multiplicity of the signals is described with the following abbreviations: s = singlet, d = doublet, t = triplet, q = quartet, dd = doublet of doublet, m = multiplet, br = broad signal. The coupling constants *J* are given in Hz. NMR spectra of the inhibitors **1-4** represent the signals of the main conformer. MS spectra were measured on a Q-Trap 2000 system with an electrospray interface (ESI). Flash column chromatography was performed on silica gel (0.04-0.063 mm, Macherey-Nagel, Düren, Germany) and was monitored by TLC on aluminium sheets (Silicagel 60 F254, Merck, Darmstadt, Germany) with UV light at 254 nm or 366 nm. Preparative HPLC was performed with a Varian HPLC system gradient system (reversed-phase column: Nucleodur C₁₈, 5 µm, 100 Å, 32 x 250 mm, Macherey-Nagel, Düren, Germany). All solvents were HPLC grade and in a gradient run the percentage of acetonitrile was increased by 0.5% solvent min⁻¹ at a flow rate of 20 mL min⁻¹. The purity of all inhibitors used for this study was at least 95% as determined by analytical HPLC with a Shimadzu LC-10A system (reversed-phase column: Nucleodur C₁₈, 5 µm, 100 Å, 4.6 x 250 mm, Macherey-Nagel, Düren, Germany). All solvents were HPLC grade and in a gradient run the percentage of acetonitrile was increased by 1% solvent min⁻¹ at a flow

rate of 1 mL min⁻¹. The detection was recorded at a wavelength of 220 nm. The inhibitors **1-4** were obtained as double TFA salts after lyophilization.

Methyl 2,6-dibromoisonicotinate (6). Citrazinic acid **5** (4.50 g, 29.0 mmol) and POBr₃ (24.9 g, 87.0 mmol) were heated to 130 °C for 0.5 h and for additional 1.5 h at 150 °C. The mixture was cooled to 0 °C and MeOH (40 mL) was added carefully. The mixture was stirred for 15 h at room temperature and the solvent was removed under reduced pressure. Saturated NaHCO₃-solution (200 mL) was added and the mixture was neutralized with solid NaHCO₃. The solution was extracted with DCM (3 x 200 mL), dried over MgSO₄, filtered and concentrated in vacuo. The residue was purified by flash column chromatography (cyclohexane/EtOAc, 11:1). **6** (6.32 g, 21.4 mmol, 74%) was obtained as a white solid. ¹H NMR (400 MHz, CDCl₃) δ = 7.99 (s, 2H), 3.97 (s, 3H). ¹³C NMR (100 MHz, CDCl₃) δ = 163.1, 141.6, 141.5, 126.8, 53.4. MS (ESI+) *m/z* calculated for C₇H₉Br₂N₂O₂ [M+NH₄]⁺: 310.90; found: 310.95.

(2,6-Dibromopyridin-4-yl)methanol (7). **6** (5.90 g, 20.0 mmol) was dissolved in MeOH (90 mL) and NaBH₄ (3.03 g, 80 mmol) was slowly added. The mixture was stirred for 3 h at 65 °C and was cooled afterwards to room temperature. 1 M HCl-solution (40 mL) was

added and the solvent was concentrated to 10 mL volume. The solution was neutralized with solid Na_2CO_3 and the mixture was stirred for additional 2 h at room temperature. The resulting precipitate was dissolved in DCM (50 mL) and diluted with H_2O (50 mL). The aqueous layer was extracted with DCM (3 x 50 mL) and the combined organic layer was dried over MgSO_4 , filtered and concentrated in vacuo. The residue was purified by flash column chromatography (cyclohexan/EtOAc, 3:1). **7** (4.86 g, 18.2 mmol, 91%) was obtained as a white solid. ^1H NMR (400 MHz, $\text{DMSO}-d_6$) δ = 7.61 (m, 2H), 5.62 (t, J = 5.8 Hz, 2H), 4.54 (d, J = 5.8 Hz, 2H). ^{13}C NMR (100 MHz, $\text{DMSO}-d_6$) δ = 158.9, 139.7, 124.6, 60.5. MS (ESI+) m/z calculated for $\text{C}_6\text{H}_9\text{Br}_2\text{N}_2\text{O}$ $[\text{M}+\text{NH}_4]^+$: 282.90; found: 282.96.

4-(Azidomethyl)-2,6-dibromopyridine (8). **7** (4.40 g, 16.6 mmol) was dissolved in 1,4-dioxane (40 mL) and PBr_3 (1.9 mL, 19.7 mmol) was added. The mixture was stirred for 3 h at 40 °C and was cooled afterwards to room temperature. Saturated NaHCO_3 -solution (100 mL) was added and the aqueous layer was extracted with DCM (3 x 100 mL). The combined organic layer was dried over MgSO_4 , filtered and the solvent was removed under reduced pressure. The crude product was dissolved in DMF (40 mL) and NaN_3 (2.14 g, 33.0 mmol) was added. The mixture was stirred for 18 h at room temperature

and was diluted with H₂O (80 mL). The solution was extracted with EtOAc (3 x 80 mL) and the combined organic layer was washed with brine. The solution was dried over MgSO₄, filtered and the solvent was removed under reduced pressure. The residue was purified by flash column chromatography (cyclohexan/EtOAc, 10:1). **8** (3.19 g, 10.9 mmol, 66% over 2 steps) was obtained as a light-yellow solid. ¹H NMR (400 MHz, DMSO-*d*₆) δ = 7.72 (s, 2H), 4.60 (s, 2H). ¹³C NMR (100 MHz, DMSO-*d*₆) δ = 151.5, 140.1, 126.2, 50.8. MS (ESI+) *m/z* calculated for C₆H₈Br₂N₅ [M+NH₄]⁺: 307.91; found: 307.95.

Tert-butyl((2,6-dibromopyridin-4-yl)methyl)carbamate (9). Azide **8** (2.73 g, 9.35 mmol) was dissolved in THF (30 mL) and a 1 M solution of PMe₃ in THF (10.3 mL, 10.3 mmol) was added at 0 °C. After 3 h stirring at room temperature, a solution of Boc₂O (2.45 g, 11.2 mmol) in THF (9 mL) was dropwise added at 0 °C and the mixture was stirred for additional 2 h. 1 M phosphate buffer (pH 7, 50 mL) was added to the mixture and the aqueous layer was extracted with DCM (3 x 70 mL). The combined organic layer was washed with brine, dried over MgSO₄, filtered and concentrated in vacuo. The residue was purified by flash column chromatography (cyclohexane/EtOAc, 6:1). **9** (1.72 g, 4.67 mmol, 50%) was obtained as a yellow solid. ¹H NMR (400 MHz, DMSO-*d*₆) δ = 7.54

(s, 2H), 4.28 (d, J = 6.1 Hz, 2H), 1.40 (s, 9H). ^{13}C NMR (100 MHz, $\text{DMSO}-d_6$) δ = 156.2, 155.7, 139.9, 125.5, 78.5, 41.7, 28.1. MS (ESI+) m/z calculated for $\text{C}_{11}\text{H}_{15}\text{Br}_2\text{N}_2\text{O}_2$ [M+H] $^+$: 364.95; found: 365.05.

Tert-butyl((2,6-diaminopyridin-4-yl)methyl)carbamate (10). **9** (1.00 g, 2.73 mmol), 25% (w/v) aqueous NH_3 -solution (8.2 mL, 109 mmol), Cu_2O (39 mg, 0.273 mmol), K_2CO_3 (76 mg, 0.546 mmol) DMEDA (29.4 μL , 0.273 mmol) was dissolved in ethylene glycol (6 mL) and stirred for 16 h at 60 $^\circ\text{C}$. The mixture was extracted with EtOAc (3 \times 25 mL) and was washed with brine. The combined organic layer was dried over MgSO_4 , filtered and the solvent was removed under reduced pressure. The residue was purified by flash column chromatography (DCM/MeOH, 9:1 + 1% (v/v) NEt_3). **10** (0.41 g, 1.72 mmol, 63%) was obtained as a yellow solid. ^1H NMR (400 MHz, $\text{DMSO}-d_6$) δ = 7.16 (t, J = 6.0 Hz, 1H), 5.52 (s, 2H), 5.29 (s, 4H), 3.82 (d, J = 6.2 Hz, 2H), 1.39 (s, 9H). ^{13}C NMR (100 MHz, $\text{DMSO}-d_6$) δ = 158.6, 155.6, 151.2, 93.5, 77.6, 42.8, 28.2. MS (ESI+) m/z calculated for $\text{C}_{11}\text{H}_{19}\text{N}_4\text{O}_2$ [M+H] $^+$: 239.15; found: 239.16.

4-(Aminomethyl)pyridine-2,6-diamine · 2 HCl (11). **10** (330 mg, 1.39 mmol) was dissolved in 1,4-dioxane (5 mL) and a 4 M solution of HCl in THF (7 mL) was added. The

1
2
3 mixture was stirred for 3 h at room temperature. The solvent was removed under reduced
4
5
6
7 pressure. **10** (279 mg, 1.32 mmol, 95%) was obtained as a white solid. ^1H NMR (400
8
9
10 MHz, $\text{DMSO}-d_6$) δ = 13.1 (s, 1H), 8.75 (s, br, 3H), 7.53 (s, 4H), 5.95 (s, 2H), 3.82 (s, 2H).
11
12
13 ^{13}C NMR (100 MHz, $\text{DMSO}-d_6$) δ = 151.8, 151.7, 94.2, 41.1. MS (ESI+) m/z calculated
14
15
16 for $\text{C}_6\text{H}_{11}\text{N}_4$ $[\text{M}+\text{H}]^+$: 139.10; found: 139.16.
17
18
19

20
21 *General Procedure for the Synthesis of the Intermediates 15-18.* Boc-D-Phe²³/D-DiPhe-
22
23
24 Pro-OH¹⁹ (1.0 eq, Boc-D-DiPhe-Pro-OH only for **14**) and amine **11-14** (1.1 eq) were
25
26
27 dissolved in DMF (5 mL), followed by the addition of $\text{HOBt} \cdot \text{H}_2\text{O}$ (1.1 eq), $\text{EDC} \cdot \text{HCl}$
28
29
30 (1.1 eq) and DIPEA (2.5-3.5 eq) at 0 °C. The mixture was stirred 16-24 h at 0 °C-rt and
31
32
33 was extracted with EtOAc (3 x 15 mL). The resulting organic solution was washed with
34
35
36 0.2 M HCl-solution (3 x 15 mL), saturated NaHCO_3 -solution (3 x 15 mL) and brine
37
38
39 (1 x 15 mL). The solvent was removed under reduced pressure and the residue was
40
41
42 purified by flash column chromatography.
43
44
45
46

47
48
49 *Boc-D-Phe-Pro derivative 15.* According to the general procedure A, compound **15** was
50
51
52 prepared using Boc-D-Phe-Pro-OH (250 mg, 0.690 mmol), amine **11** (160 mg,
53
54
55 0.759 mmol), $\text{HOBt} \cdot \text{H}_2\text{O}$ (116 mg, 0.759 mmol), $\text{EDC} \cdot \text{HCl}$ (146 mg, 0.759 mmol) and
56
57
58
59
60

DIPEA (0.42 mL, 2.41 mmol). The crude product was purified by flash column chromatography (DCM/MeOH, 8:1). **15** (259 mg, 0.537 mmol, 78%) was obtained as a yellow solid. ^1H NMR (400 MHz, DMSO- d_6) δ = 7.81 (t, J = 6.0 Hz, 1H), 7.29-7.14 (m, 6H), 5.59-5.51 (m, 6H), 4.39-4.24 (m, 2H), 4.06-3.84 (m, 2H), 3.61-3.44 (m, 1H), 3.03-2.67 (m, 3H), 1.91-1.74 (m, 3H), 1.67-1.59 (m, 1H), 1.31 (s, 9H). ^{13}C NMR (100 MHz, DMSO- d_6) δ = 171.0, 170.3, 157.7, 155.4, 151.1, 138.4, 137.1, 129.3, 128.0, 126.4, 93.4, 78.3, 59.8, 53.8, 46.3, 41.4, 36.9, 29.0, 28.1, 23.9. MS (ESI+) m/z calculated for $\text{C}_{25}\text{H}_{35}\text{N}_6\text{O}_4$ $[\text{M}+\text{H}]^+$: 483.27; found: 483.35.

Boc-D-Phe-Pro derivative 16. According to the general procedure A, compound **16** was prepared using Boc-D-Phe-Pro-OH (200 mg, 0.552 mmol), amine **12** (commercially available from ChemPur, 136 mg, 0.607 mmol), $\text{HOBt} \cdot \text{H}_2\text{O}$ (93 mg, 0.607 mmol), EDC \cdot HCl (116 mg, 0.607 mmol) and DIPEA (0.24 mL, 1.38 mmol). The crude product was purified by flash column chromatography (cyclohexane/EtOAc, 1:3). **16** (229 mg, 0.403 mmol, 73%) was obtained as a colorless solid. ^1H NMR (400 MHz, DMSO- d_6) δ = 9.65 (s, 1H), 8.13-8.10 (m, 1H), 8.00 (t, J = 6.1 Hz, 1H), 7.67 (s, 1H), 7.29-7.12 (m, 6H), 6.91-6.88 (m, 1H), 4.43-4.25 (m, 3H), 3.64-3.44 (m, 1H), 3.03-2.92 (m, 1H), 2.92-2.81 (m,

2H), 2.81-2.73 (m, 1H), 1.92-1.80 (m, 3H), 1.69-1.60 (m, 1H), 1.46 (s, 9H), 1.25 (s, 9H).

^{13}C NMR (100 MHz, DMSO- d_6) δ = 171.3, 170.5, 155.4, 152.6, 152.4, 150.2, 147.5, 137.2, 129.3, 128.0, 126.4, 116.3, 109.9, 79.4, 78.3, 59.9, 53.8, 46.4, 41.3, 36.9, 28.9, 28.0, 27.9, 23.8. MS (ESI+) m/z calculated for $\text{C}_{30}\text{H}_{42}\text{N}_5\text{O}_6$ $[\text{M}+\text{H}]^+$: 568.32; found: 568.37.

Boc-D-Phe-Pro derivative 17. According to the general procedure A, compound **17** was prepared using Boc-D-Phe-Pro-OH (200 mg, 0.552 mmol), amine **13** (commercially available from ChemPur, 136 mg, 0.607 mmol), HOBt·H₂O (93 mg, 0.607 mmol), EDC·HCl (116 mg, 0.607 mmol) and DIPEA (0.24 mL, 1.38 mmol). The crude product was purified by flash column chromatography (cyclohexane/EtOAc, 1:4). **17** (205 mg, 0.361 mmol, 65%) was obtained as a colorless solid. ^1H NMR (400 MHz, DMSO- d_6) δ = 9.63 (s, 1H), 8.17-8.09 (m, 1H), 7.94 (t, J = 5.9 Hz, 1H), 7.70 (s, 1H), 7.29-7.19 (m, 6H), 7.09-7.07 (m, 1H), 4.43-4.22 (m, 3H), 3.61-3.43 (m, 1H), 3.03-2.97 (m, 1H), 2.92-2.79 (m, 2H), 2.73-2.72 (m, 1H), 1.85-1.71 (m, 3H), 1.65-1.68 (m, 1H), 1.47 (s, 9H), 1.27 (s, 9H). ^{13}C NMR (100 MHz, DMSO- d_6) δ = 171.2, 170.5, 155.4, 152.6, 151.1, 146.8, 146.1, 137.2, 136.5, 129.3, 128.0, 126.4, 111.8, 79.4, 78.3, 59.9, 53.8, 46.4, 36.9, 29.0, 27.9, 23.9. MS (ESI+) m/z calculated for $\text{C}_{30}\text{H}_{42}\text{N}_5\text{O}_6$ $[\text{M}+\text{H}]^+$: 568.32; found: 568.46.

Boc-D-DiPhe-Pro derivative 18. According to the general procedure A, compound **18** was prepared using Boc-D-DiPhe-Pro-OH (270 mg, 0.616 mmol), amine **14** (commercially available from Sigma Aldrich, 47 μ L, 0.677 mmol), HOBt \cdot H₂O (104 mg, 0.677 mmol), EDC \cdot HCl (130 mg, 0.677 mmol) and DIPEA (0.26 mL, 1.54 mmol). The crude product was purified by flash column chromatography (DCM/MeOH, 11:1). **18** (246 mg, 0.465 mmol, 76%) was obtained as a colorless solid. ¹H NMR (400 MHz, DMSO-*d*₆) δ = 8.47-8.46 (m, 2H), 8.04 (t, *J* = 6.1 Hz, 1H), 7.41-7.39 (m, 2H), 7.31-7.16 (m, 11H), 7.09-7.07 (m, 1H), 5.13-5.08 (m, 1H), 4.39 (d, *J* = 11.6 Hz, 1H), 4.27 (d, *J* = 6.1 Hz, 2H), 3.96-3.93 (m, 1H), 3.74-2.68 (m, 1H), 3.13-3.07 (m, 1H), 1.80-1.69 (m, 2H), 1.56-1.42 (m, 2H), 1.18 (s, 9H). ¹³C NMR (100 MHz, DMSO-*d*₆) δ = 172.0, 170.5, 156.1, 149.9, 148.8, 141.3, 141.2, 129.3, 128.9, 128.6, 127.2, 126.8, 122.2, 78.8, 59.9, 55.0, 53.2, 47.2, 41.5, 29.4, 28.5, 24.4. MS (ESI+) *m/z* calculated for C₃₁H₃₇N₄O₄ [M+H]⁺: 529.28; found: 529.46.

General Procedure for the Synthesis of the Inhibitors 1-4. Compound **15-18** (1.0 eq) was dissolved in TFA (10 eq.). The mixture was stirred for 2 h and concentrated in vacuo. The residue was purified by preparative HPLC.

D-Phe-Pro inhibitor 1. According to the general procedure B, inhibitor **1** was prepared using compound **15** (97.0 mg, 0.200 mmol) and TFA (2 mL). The crude product was purified by preparative HPLC. **1** (96.0 mg, 0.157 mmol, 78%) was obtained as a white solid. ^1H NMR (500 MHz, $\text{DMSO-}d_6$) δ = 12.8 (s, 1H), 8.42-8.40 (m, 3H), 7.37-7.23 (m, 6H), 7.19 (s, 4H), 5.76 (s, 2H), 4.39-4.30 (m, 1H), 4.20-4.18 (m, 1H), 4.09-3.99 (m, 2H), 3.54-3.50 (m, 1H), 3.12 (dd, J = 13.1, J = 5.8 Hz, 1H), 2.97 (dd, J = 13.1, J = 9.0 Hz, 1H), 2.65-2.60 (m, 1H), 1.83-1.70 (m, 3H), 1.44 (m, 1H). ^{13}C NMR (126 MHz, $\text{DMSO-}d_6$) δ = 171.2, 167.0, 158.7 (q, J = 33.3 Hz), 158.2, 151.7, 134.5, 129.4, 128.5, 127.4, 116.6 (q, J = 296.5 Hz), 92.9, 60.0, 52.0, 46.6, 41.3, 36.7, 29.2, 23.7. MS (ESI+) m/z calculated for $\text{C}_{20}\text{H}_{27}\text{N}_6\text{O}_2$ $[\text{M}+\text{H}]^+$: 383.22; found: 383.22.

D-Phe-Pro inhibitor 2. According to the general procedure B, inhibitor **2** was prepared using compound **16** (171 mg, 0.301 mmol) and TFA (3 mL). The crude product was purified by preparative HPLC. **2** (165 mg, 0.280 mmol, 92%) was obtained as a white solid. ^1H NMR (500 MHz, $\text{DMSO-}d_6$) δ = 13.9 (s, br, 1H), 8.52 (t, J = 6.0 Hz, 1H), 8.36 (s, br, 3H), 8.13 (s, br, 2H), 7.86-7.85 (m, 1H), 7.37-7.28 (m, 3H), 7.25-7.23 (m, 2H), 6.78-6.77 (m, 1H), 6.73 (dd, J = 6.6 Hz, J = 1.6 Hz, 1H), 4.40-4.34 (m, 1H), 4.26 (d, J = 5.9 Hz,

2H), 4.22-4.20 (m, 1H), 3.53-3.49 (m, 1H), 3.12 (dd, $J = 13.2$, $J = 5.9$ Hz, 1H), 2.98 (dd, $J = 13.1$, $J = 8.7$ Hz, 1H), 2.69-2.64 (m, 1H), 1.88-1.71 (m, 3H), 1.49-1.42 (m, 1H). ^{13}C NMR (126 MHz, DMSO- d_6) $\delta = 171.4$, 167.0, 158.6 (q, $J = 33.6$ Hz), 158.2, 157.2, 154.0, 135.5, 134.4, 129.4, 128.5, 127.4, 116.4 (q, $J = 296.0$ Hz), 110.9, 109.5, 60.0, 52.0, 46.6, 41.3, 36.7, 29.2, 23.8. MS (ESI+) m/z calculated for $\text{C}_{20}\text{H}_{26}\text{N}_5\text{O}_2$ $[\text{M}+\text{H}]^+$: 368.21; found: 368.23.

D-Phe-Pro inhibitor 3. According to the general procedure B, inhibitor **3** was prepared using compound **17** (135 mg, 0.238 mmol) and TFA (2.4 mL). The crude product was purified by preparative HPLC. **3** (109 mg, 0.109 mmol, 82%) was obtained as a white solid. ^1H NMR (400 MHz, DMSO- d_6) $\delta = 8.40$ (t, $J = 5.9$ Hz, 1H), 8.27 (s, br, 3H), 8.03 (s, br, 2H), 7.79-7.77 (m, 2H), 7.37-7.27 (m, 3H), 7.24-7.22 (m, 2H), 6.94-6.92 (m, 1H), 4.39-4.32 (m, 1H), 4.17-4.13 (m, 3H), 3.54-3.48 (m, 1H), 3.08 (dd, $J = 13.3$, $J = 6.1$ Hz, 1H), 2.97 (dd, $J = 13.2$, $J = 8.5$ Hz, 1H), 2.74-2.67 (m, 1H), 1.84-1.70 (m, 3H), 1.47-1.40 (m, 1H). ^{13}C NMR (126 MHz, DMSO- d_6) $\delta = 171.2$, 167.0, 158.6 (q, $J = 34.4$ Hz), 153.4, 143.7, 134.4, 133.2, 129.4, 128.5, 127.4, 123.5, 116.2 (q, $J = 294.3$ Hz), 113.4, 60.0,

52.0, 46.6, 38.3, 36.6, 29.1, 23.7. MS (ESI+) m/z calculated for $C_{20}H_{26}N_5O_2$ $[M+H]^+$: 368.21; found: 368.25.

D-DiPhe-Pro inhibitor 4. According to the general procedure B, inhibitor **4** was prepared using compound **18** (159 mg, 0.301 mmol) and TFA (3 mL). The crude product was purified by preparative HPLC. **4** (182 mg, 0.277 mmol, 92%) was obtained as a colorless solid. 1H NMR (500 MHz, DMSO- d_6) δ = 8.77 (d, J = 6.3 Hz, 2H), 8.54 (t, J = 6.0 Hz, 1H), 8.35 (s, br, 3H), 7.79 (d, J = 6.4 Hz, 2H), 7.66-7.65 (m, 2H), 7.45-7.42 (m, 2H), 7.36-7.24 (m, 6H), 5.02 (d, J = 11.2 Hz, 1H), 4.53 (dd, J = 17.6, J = 6.3 Hz, 1H), 4.45 (dd, J = 17.6, J = 5.7 Hz, 1H), 4.40 (d, J = 11.2 Hz, 1H), 3.61-3.57 (m, 1H), 2.93-2.88 (m, 1H), 1.77-1.68 (m, 2H), 1.57-1.48 (m, 1H), 1.29-1.22 (m, 1H). ^{13}C NMR (126 MHz, DMSO- d_6) δ = 171.3, 167.1, 158.4 (q, J = 35.0 Hz), 157.6, 143.0, 138.4, 137.5, 129.0, 128.9, 128.3, 127.6, 127.5, 123.9, 116.2 (q, J = 293.8 Hz), 60.0, 53.5, 53.3, 47.1, 41.5, 28.9, 23.6. MS (ESI+) m/z calculated for $C_{26}H_{29}N_4O_2$ $[M+H]^+$: 429.23; found: 429.29.

pK_a Determination. The ionization constant pK_a of the compounds of interest were determined by SiriusT3 pH-metric pK_a method, which is based on the potentiometric titration method reported in reference.⁴⁹ For the titration approx. 1.0 mg of solid sample

was weighed into a vial and dissolved in 1.5 mL of water containing 0.15 M KCl as background electrolyte. The electrolyte serves to improve the measurement precision and to mimic the physiological state. The pH of the dilute sample solution was adjusted to pH 2.0 by addition of 0.5 M HCl and then titrated with standardized base (0.5 M KOH) to pH 12.0 at 25 °C under argon atmosphere. During the titration more than 25 pH readings (volume of titrant vs. pH) were collected and compared with a blank titration (without sample). The resulted shape of the curve indicates the amount of substance present and its characteristic acid–base ionization properties. pK_a results were calculated by SIRIUS T3 Refine Version 1.1.

ITC Data Collection. All ITC experiments were performed on a Microcal ITC₂₀₀ (Malvern) device at 25 °C with a reference power of 5 $\mu\text{cal s}^{-1}$. To determine the thermodynamic profiles including protonation effects in thrombin, a direct titration was used for all four ligands. Ligand solutions of 0.4 mM **1**, 0.6 mM **2**, 0.3 mM **3** and 1.5 mM **4** were titrated into 40, 60, 30 or 150 μM thrombin, respectively. Thrombin samples were prepared by a solution of human α -thrombin (Beriplast®, CSL Behring, Marburg, Germany) in a buffer of 100 mM NaCl, 0.1% (w/v) PEG8000 and 50 mM phosphate, HEPES, Tricine or Tris at pH

7.8 which was dialyzed at 4 °C overnight. Ligands were dissolved in the same buffer with 3% (v/v) DMSO in order to assure a complete solubility. The titration protocol consisted of an initial volume of 0.3 μ L and 12-22 injections between 1.3-1.5 μ L separated by an interval of 180 s. To collect the ITC data for trypsin, two titration protocols were used. The direct direction was performed for **1-3** with a ligand concentration of 2.5 mM, which were titrated into 125 μ M trypsin to determine the protonation states whereas a displacement titration was used for ligand **4** due to its lower affinity toward trypsin. Trypsin samples were prepared by a solution of bovine- β -trypsin (Sigma Aldrich, product number T8003) in a buffer of 80 mM NaCl, 10 mM CaCl₂, 0.1% (w/v) PEG8000 and 100 mM HEPES, Tricine or Tris at pH 7.8 which was dialyzed at 4 °C overnight. Ligands were dissolved in the same buffer with 3% (v/v) DMSO in order to support a complete solubility as for the ligand preparation in thrombin. An initial volume of 0.3 μ L was followed by 28-30 injections with a volume of 1.1 μ L using 180 s as interval time for the direct titration while 19 injections were chosen with 1.9 μ L volume and the same interval time for the displacement titration. According to this, 40 μ M trypsin was pre-incubated with 3.4 mM of **4** using compound **19** (Table S3) as a displacement ligand with a concentration 0.4 mM.

The displacement ligand **19** was analyzed in a direct measurement with a ligand concentration of 0.3 mM, which was titrated into 30 μ M trypsin. To confirm the dissociation constants K_d of **1-3** from the direct titrations, the displacement titration was additionally performed in 40 μ M trypsin (pre-incubated with 0.22 mM **1**, 0.45 mM **2** or 0.35 mM **3**) after the same procedure as above. The ligand concentrations for the pre-incubation of the protein were calculated according to a previous study in order to reach a saturation goal of 87%, which is based on the K_i values from the fluorescence assay. All ITC titrations were performed at least in triplicate and the raw thermograms were analyzed with *NITPIC*⁵⁰ (version 1.1.8) and *SEDPHAT*⁵¹ (version 10.58d).

Crystallization. Human α -thrombin (Enzyme Research Laboratories, South Bend, IN, USA) was dissolved in a crystallization buffer consisting of 20 mM NaH_2PO_4 (pH 7.5), 350 mM NaCl and 2 mM benzamidine at a concentration of 10 mg mL^{-1} . A hirudin fragment (residues 54-65, Bachem, Bubendorf, Switzerland) was dissolved in the crystallization buffer at 2.5 mg mL^{-1} . The two solutions were mixed in a ratio of 80% thrombin solution and 20% hirudin solution. The mixture was incubated for 1 h at 4 $^{\circ}\text{C}$ and centrifuged for 5 min. Thrombin crystals were grown at 4 $^{\circ}\text{C}$ by the hanging-drop

vapor diffusion method in 2 μL crystallization drops, respectively. 1 μL of the mixture thrombin-hirudin was placed on a cover slide with 1 μL of reservoir buffer composed of 20 mM NaH_2PO_4 (pH 7.5), 350 mM NaCl, 27% (w/v) PEG 8000 followed by microseeding. After three weeks thrombin crystals were obtained in good diffracting quality for soaking. The soaking solution (50% crystallization buffer and 50% reservoir buffer) was combined with the ligand solution in a final concentration of 5 mM ligand and 10% DMSO. The crystals were soaked for 24 h remaining at 4 $^\circ\text{C}$ and were flash-frozen in liquid nitrogen in a cryoprotectant solution of reservoir buffer, 20% glycerol and 5 mM of the respective ligand.

Bovine- β -trypsin was dissolved at a concentration of 20 mg mL^{-1} in 10 mM CaCl_2 , 1 mM HCl, 3 mM **1-3** or 6 mM **4** and 6% (v/v) DMSO. Trypsin crystals were grown at 18 $^\circ\text{C}$ on sitting-drop plates in 2 μL crystallization drops, respectively. Each crystallization drop consisted of 1 μL trypsin-ligand solution and 1 μL reservoir buffer which contained 0.1 M imidazole, 0.1 M $(\text{NH}_4)_2\text{SO}_4$, 0.1% (w/v) NaN_3 and 25-27% (w/v) PEG8000 at pH 7-8. The crystals finished growing after 7 days and were flash-frozen in liquid nitrogen in a

cryoprotectant solution composed of reservoir buffer, 20% glycerol and 3-6 mM of the respective ligand.

X-ray Data Collection, Structure Determination and Refinement. The data collection of all crystals was performed on beamline 14.1 or 14.2 at BESSY II (Berlin, Germany) or on EMBL beamline P13 at DESY (Hamburg, Germany) which are both equipped with a Dectris Pilatus 6M detector or Marmosaic 225. The data were processed using *XDS*⁵² and *XDSAPP2.0*.⁵³ The starting model was generated by molecular replacement using *Phaser* (version 2.5.7-2.7.17)⁵⁴ with the PDB structures 2ZGB or 1H8D for thrombin and 5MNK for trypsin as search models. The structures were refined using *Phenix.refine* (version 1.10.1-1.15.2)⁵⁵ against structure factor amplitudes in five cycles for each refinement. *Coot* (version 0.7.2-0.8.9.1)⁵⁶ was used to generate and to build a model into σ -weighted maps ($2mF_o-DF_c$ and mF_o-DF_o). Simulated annealing was performed in the first step to remove potential bias from the search model. Thrombin structures with inhibitor **2** and **3** were refined anisotropically, whereas the complexes with inhibitor **1** and **4** were refined isotropically. TLS parameters were used subsequently to these isotropic refinements, whereupon the definition of the TLS groups was done with Phenix. For the

trypsin complex structure with inhibitor **1**, the *B*-factors were refined isotropically with TLS groups. In all remaining trypsin structures, anisotropic *B*-factor refinement was applied. Multiple sidechain conformations, water molecules, ions, solvents and ligands were built into the model and maintained during the refinement if the minor populated side chain displayed at least 20% occupancy. Further data and refinement statistics are described in Tables 5 and 6.

Table 5. X-ray Data Collection and Refinement Statistics for Thrombin Structures of 1-4.

	Ligand (PDB code)			
	1 (6HSX)	2 (6T3Q)	3 (6T4A)	4 (6TDT)
Data Collection and Processing				
Wavelength (Å)	0.9184	0.9184	0.9184	0.9184
Beamline	BESSY, 14.1	BESSY, 14.2	BESSY, 14.2	BESSY, 14.1
Detector	PILATUS 6M	Marmosaic 225 mm	Marmosaic 225 mm	PILATUS 6M
Space group	C121	C121	C121	C121
Unit cell parameters:				
a, b, c (Å)	70.0, 71.7, 72.6	70.0, 71.3, 72.6	70.2, 71.3, 72.5	70.0, 71.7, 72.1
α, β, γ (°)	90.0, 100.4, 90.0	90.0, 100.6, 90.0	90.0, 100.6, 90.0	90.0, 100.2, 90.0
Matthews coefficient (Å ³ /Da)	2.5	2.5	2.5	2.5
Solvent content (%)	52	51	51	51
Diffraction Data^a				
Resolution range (Å)	43.50-1.56 (1.59-1.56)	50.00-1.33 (1.35-1.33)	50.00-1.31 (1.33-1.31)	43.36-1.53 (1.62-1.53)
Unique reflections	49365 (7727)	80331 (4048)	84043 (4191)	52277 (8431)
Redundancy	3.4 (3.5)	3.8 (3.5)	3.3 (3.2)	3.4 (3.5)
<i>R</i> (<i>I</i>) _{sym} (%)	4.0 (49.0)	4.6 (49.5)	4.3 (43.2)	8.5 (47.3)

Wilson B factor (Å ²)	19.6	11.8	11.1	15.5
Completeness (%)	97.6 (95.2)	100 (100)	99.9 (99.9)	98.7 (98.9)
<I/σ(I)>	17.4 (2.5)	26.8 (2.6)	26.7 (2.7)	8.6 (2.1)
Refinement				
Resolution range (Å)	43.51-1.56	18.51-1.33	35.63-1.31	43.36-1.53
Reflections (work/free)	46896 / 2469	76296 / 4035	79852 / 4189	49662 / 2611
Final R value for all reflections (work/free) (%)	16.2 / 18.4	12.5 / 14.6	12.7 / 14.8	16.1 / 17.7
Protein residues (L chain / H chain)	28 / 250	29 / 251	28 / 251	31 / 251
Residues of hirudin (I chain)	11	10	10	11
Sodium atoms	2	2	2	2
Inhibitor atoms	28	35	27	32
Water molecules	229	257	262	253
RMSD from ideality:				
Bond lengths (Å)	0.008	0.007	0.006	0.008
Bond angles (°)	0.993	1.046	0.994	1.030
Ramachandran plot (%) ^b :				
Most favored regions	86.1	87.0	85.7	87.9
Additionally allowed regions	13.5	12.6	14.3	11.7
Generously allowed regions	0.4	0.4	0.0	0.4
Disallowed regions	0.0	0.0	0.0	0.0
Mean B factors (Å ²) ^c :				
Protein (L chain + H chain)	26.6	17.0	15.9	19.7
Ligand	20.1	12.1	11.4	19.5
Water molecules	33.7	28.4	26.8	27.0

^aValues in parenthesis refer to the highest resolution shell
^bCalculated using PROCHECK⁵⁷
^cCalculated using MOLEMAN excluding hydrogen atoms^{58,59}

Table 6. X-ray Data Collection and Refinement Statistics for Trypsin Structures of 1-4.

Ligand (PDB code)				
1 (6T0M)	2 (6T3Q)	3 (6T5W)	4 (6SY3)	

Data Collection and Processing

Wavelength (Å)	0.9763	0.9763	0.9184	0.9184
Beamline	DESY, P13	DESY, P13	BESSY, 14.1	BESSY, 14.1
Detector	PILATUS 6M-F	PILATUS 6M-F	PILATUS 6M	PILATUS 6M
Space group	P2 ₁ 2 ₁ 2 ₁	P2 ₁ 2 ₁ 2 ₁	P2 ₁ 2 ₁ 2 ₁	P2 ₁ 2 ₁ 2 ₁
Unit cell parameters:				
a, b, c (Å)	54.5, 56.8, 66.7	54.6, 56.7, 66.7	54.2, 56.8, 66.2	54.5, 58.5, 66.6
α, β, γ (°)	90.0, 90.0, 90.0	90.0, 90.0, 90.0	90.0, 90.0, 90.0	90.0, 90.0, 90.0
Matthews coefficient (Å ³ /Da)	2.0	2.0	2.0	2.2
Solvent content (%)	38	38	38	44

Diffraction Data^a

Resolution range (Å)	43.22-1.51 (1.60-1.51)	43.18-1.19 (1.26-1.19)	43.12-1.13 (1.35-1.33)	43.10-0.95 (1.01-0.95)
Unique reflections	33113 (5172)	66940 (10620)	76852 (12065)	127398 (19451)
Redundancy	5.8 (5.6)	5.7 (5.7)	5.0 (4.8)	4.1 (3.2)
$R(I)_{\text{sym}}$ (%)	5.5 (48.7)	5.3 (49.2)	5.2 (56.5)	3.8 (49.1)
Wilson B factor (Å ²)	16.0	12.6	11.3	8.7
Completeness (%)	99.4 (97.5)	99.6 (98.9)	99.5 (97.8)	98.0 (93.3)
$\langle I/\sigma(I) \rangle$	17.5 (3.1)	15.0 (2.8)	14.6 (2.6)	16.0 (1.8)

Refinement

Resolution range (Å)	43.22-1.51	42.22-1.19	43.11-1.13	33.80-0.95
Reflections (work/free)	31457 / 1655	63593 / 3347	73009 / 3843	125174 / 2224
Final R value for all reflections (work/free) (%)	14.8 / 17.1	12.3 / 13.9	12.8 / 14.5	12.4 / 13.4
Protein residues	223	223	223	223
Calcium atoms	1	1	1	1
Inhibitor atoms	28	27	36	32
Water molecules	173	202	201	233
RMSD from ideality:				
Bond lengths (Å)	0.007	0.006	0.005	0.005
Bond angles (°)	0.935	0.906	0.903	0.944
Ramachandran plot (%) ^b :				
Most favored regions	86.2	87.2	85.6	86.7
Additionally allowed regions	13.8	12.8	14.4	13.3
Generously allowed regions	0.0	0.0	0.0	0.0

1
2
3
4
5
6
7
8
9
10
11
12
13
14
15
16
17
18
19
20
21
22
23
24
25
26
27
28
29
30
31
32
33
34
35
36
37
38
39
40
41
42
43
44
45
46
47
48
49
50
51
52
53
54
55
56
57
58
59
60

Disallowed regions	0.0	0.0	0.0	0.0
Mean B factors (Å ²) ^c :				
Protein	17.4	14.0	12.8	10.5
Ligand	21.4	15.2	11.4	10.9
Water molecules	28.5	27.4	26.1	23.6

^aValues in parenthesis refer to the highest resolution shell
^bCalculated using PROCHECK⁵⁷
^cCalculated using MOLEMAN excluding hydrogen atoms^{58,59}

ASSOCIATED CONTENT

Supporting Information

The Supporting Information is available free of charge on the ACS Publications website at DOI: 10.1021/acs.jmedchem.xxxxx

Figures of mF_o-DF_c omit maps of the investigated ligands; Reference to the numbering of water molecules in the pdb files and the manuscript; ITC results from individual titrations; Thermograms and binding isotherms from ITC measurements (PDF); HPLC traces, Molecular formula strings (CSV).

Accession Codes

Coordinates and structure factors have been deposited in the Protein Data Bank and will be released upon article publication: **1** (6HSX), **2** (6T3Q), **3** (6T4A) and **4** (6TDT) for thrombin; **1** (6T0M), **2** (6T0P), **3** (6T5W) and **4** (6SY3) for trypsin.

AUTHOR INFORMATION

Corresponding Author

*Mail: klebe@staff.uni-marburg.de; phone: +49 6421 28 21313

ORCID

Khang Ngo: [0000-0002-7561-7975](https://orcid.org/0000-0002-7561-7975)

Andreas Heine: [0000-0002-5285-4089](https://orcid.org/0000-0002-5285-4089)

Gerhard Klebe: [0000-0002-4913-390X](https://orcid.org/0000-0002-4913-390X)

Notes

The authors declare no competing financial interest.

ACKNOWLEDGMENTS

We thank CSL Behring (Marburg, Germany) for supplying human thrombin from the production of Beriplast. We are also thankful to the beamline staff at BESSY II (Helmholtz-

Zentrum Berlin, Germany) and PETRA III (EMBL Hamburg, Germany) for their support during data collection. We acknowledge the receipt of a travel grant from the Helmholtz-Zentrum Berlin. We would also like to thank Namir Abazi (Univ. of Marburg, Germany) for his support in the crystallization of thrombin. We kindly thank Prof. Dr. Torsten Steinmetzer (Univ. of Marburg, Germany) for his thorough proofreading and many valuable comments to improve the manuscript and his group for support in the enzyme kinetic fluorescence assay.

ABBREVIATIONS

AMC, 7-amido-4-methylcoumarin; HEPES, 4-(2-hydroxyethyl)-1-piperazineethanesulfonic acid; ESI, electron spray ionization; HPLC, high performance liquid chromatography; ITC, isothermal titration calorimetry; MS mass spectroscopy; NMR, nuclear magnetic resonance spectroscopy; PEG, polyethylene glycol; PK, pharmacokinetic; TLC, thin layer chromatography; Tricine, *N*-(tri(hydroxymethyl)methyl)glycine; Tris, tris(hydroxymethyl)aminomethane

REFERENCES

- (1) Hopkins, A. L.; Mason, J. S.; Overington, J. P. Can We Rationally Design Promiscuous Drugs? *Curr. Opin. Struct. Biol.* **2006**, *16*, 127–136.
- (2) Huggins, D. J.; Sherman, W.; Tidor, B. Rational Approaches to Improving Selectivity in Drug Design. *J. Med. Chem.* **2012**, *55*(4), 1424–1444.
- (3) Alterio, V.; Di Fiore, A.; D'Ambrosio, K.; Supuran, C. T.; De Simone, G. Multiple Binding Modes of Inhibitors to Carbonic Anhydrases: How to Design Specific Drugs Targeting 15 Different Isoforms? *Chem. Rev.* **2012**, *112*(8), 4421–4468.
- (4) Whitesides, G. M.; Krishnamurthy, V. M. Designing Ligands to Bind Proteins. *Q. Rev. Biophys.* **2005**, *38*(4), 385–395.
- (5) Ortiz, A.; Gomez-Puertas, P.; Leo-Macias, A.; Lopez-Romero, P.; Lopez-Vinas, E.; Morreale, A.; Murcia, M.; Wang, K. Computational Approaches to Model Ligand Selectivity in Drug Design. *Curr. Top. Med. Chem.* **2006**, *6*(1), 41–55.
- (6) Kawasaki, Y.; Freire, E. Finding a Better Path to Drug Selectivity. *Drug Discov. Today* **2011**, *16*(21–22), 985–990.

- (7) Klebe, G. *Drug Design*, Spektrum: Berlin Heidelberg, **2013**.
- (8) Krimmer, S. G.; Klebe, G. Thermodynamics of Protein-Ligand Interactions as a Reference for Computational Analysis: How to Assess Accuracy, Reliability and Relevance of Experimental Data. *J. Comput. Aided. Mol. Des.* **2015**, *29* (9), 867–883.
- (9) Betz, M.; Wulsdorf, T.; Krimmer, S. G.; Klebe, G. Impact of Surface Water Layers on Protein-Ligand Binding: How Well Are Experimental Data Reproduced by Molecular Dynamics Simulations in a Thermolysin Test Case? *J. Chem. Inf. Model.* **2016**, *56* (1), 223–233.
- (10) Ladbury, J. E. Just Add Water! The Effect of Water on the Specificity of Protein-Ligand Binding Sites and Its Potential Application to Drug Design. *Chem. Biol.* **1996**, *3* (12), 973–980.
- (11) Levy, Y.; Onuchic, J. N. Water Mediation in Protein Folding and Molecular Recognition. *Annu. Rev. Biophys. Biomol. Struct.* **2006**, *35*, 389–415.

- (12) Guvench, O.; Price, D. J.; Brooks, C. L. Receptor Rigidity and Ligand Mobility in Trypsin-Ligand Complexes. *Proteins Struct. Funct. Genet.* **2005**, *58* (2), 407–417.
- (13) Wu, E. L.; Han, K. L.; Zhang, J. Z. H. Selectivity of Neutral/Weakly Basic P1 Group Inhibitors of Thrombin and Trypsin by a Molecular Dynamics Study. *Chem. Eur. J.* **2008**, *14* (28), 8704–8714.
- (14) Hilpert, K.; Ackermann, J.; Banner, D. W.; Gast, A.; Gubernator, K.; Hadváry, P.; Labler, L.; Müller, K.; Schmid, G.; Tschopp, T. B.; van de Waterbeemd, H. Design and Synthesis of Potent and Highly Selective Thrombin Inhibitors. *J. Med. Chem.* **1994**, *37* (23), 3889–3901.
- (15) Mackman, R. L.; Katz, B. A.; Breitenbucher, J. G.; Hui, H. C.; Verner, E.; Luong, C.; Liu, L.; Sprengeler, P. A. Exploiting Subsite S1 of Trypsin-like Serine Proteases for Selectivity: Potent and Selective Inhibitors of Urokinase-Type Plasminogen Activator. *J. Med. Chem.* **2001**, *44* (23), 3856–3871.
- (16) Sichler, K.; Hopfner, K. P.; Kopetzki, E.; Huber, R.; Bode, W.; Brandstetter, H. The Influence of Residue 190 in the S1 Site of Trypsin-like Serine Proteases on

- Substrate Selectivity Is Universally Conserved. *FEBS Lett.* **2002**, *530* (1–3), 220–224.
- (17) Lobo, A. P.; Wos, J. D.; Yu, S. M.; Lawson, W. B. Active Site Studies of Human Thrombin and Bovine Trypsin: Peptide Substrates. *Arch. Biochem. Biophys.* **1976**, *177* (1), 235–244.
- (18) Gallwitz, M.; Enoksson, M.; Thorpe, M.; Hellman, L. The Extended Cleavage Specificity of Human Thrombin. *PLoS One* **2012**, *7* (2), e31756.
- (19) Baum, B.; Mohamed, M.; Zayed, M.; Gerlach, C.; Heine, A.; Hangauer, D.; Klebe, G. More than a Simple Lipophilic Contact: A Detailed Thermodynamic Analysis of Nonbasic Residues in the S1 Pocket of Thrombin. *J. Mol. Biol.* **2009**, *390* (1), 56–69.
- (20) Baum, B.; Muley, L.; Heine, A.; Smolinski, M.; Hangauer, D.; Klebe, G. Think Twice: Understanding the High Potency of Bis(Phenyl)Methane Inhibitors of Thrombin. *J. Mol. Biol.* **2009**, *391* (3), 552–564.

- (21) Biela, A.; Khayat, M.; Tan, H.; Kong, J.; Heine, A.; Hangauer, D.; Klebe, G. Impact of Ligand and Protein Desolvation on Ligand Binding to the S1 Pocket of Thrombin. *J. Mol. Biol.* **2012**, *418* (5), 350–366.
- (22) Feng, D. M.; Gardell, S. J.; Lewis, S. D.; Bock, M. G.; Chen, Z.; Freidinger, R. M.; Naylor-Olsen, A. M.; Ramjit, H. G.; Woltmann, R.; Baskin, E. P.; Lynch, J. J.; Lucas, R.; Shafer, J.A.; Dancheck, K. B.; Chen, I-W.; Mao, S.-S.; Krueger, J. A.; Hare, T. R.; Mulichak, A. M.; Vacca, J. P. Discovery of a Novel, Selective, and Orally Bioavailable Class of Thrombin Inhibitors Incorporating Aminopyridyl Moieties at the P1 Position. *J. Med. Chem.* **1997**, *40* (23), 3726–3733.
- (23) Steinmetzer, T.; Zhu, B. Y.; Konishi, Y. Potent Bivalent Thrombin Inhibitors: Replacement of the Scissile Peptide Bond at P1-P1' with Arginyl Ketomethylene Isosteres. *J. Med. Chem.* **1999**, *42* (16), 3109–3115.
- (24) Brodbeck, B.; Nettekoven, M. H. Substituted[1,2,4]Triazolo[1,5A]Pyridine Derivatives with Activity as Adenosine Receptor Ligands U.S. Patent 6,506,772 B1, **2003**.

- (25) Meredith, E. L.; Beattie, K.; Burgis, R.; Capparelli, M.; Chapo, J.; DiPietro, L.; Gamber, G.; Enyedy, I.; Hood, D. B.; Hosagrahara, V.; Jewell C; Koch K.A.; Lee W.; Lemon D. D.; McKinsey T. A.; Miranda K.; Pagratis N.; Phan D.; Plato C.; Rao C.; Rozhitskaya O.; Soldermann N.; Springer C.; van Eis M.; Vega R. B.; Yan W.; Zhu Q.; Monovich L. G. Identification of Potent and Selective Amidobipyridyl Inhibitors of Protein Kinase D. *J. Med. Chem.* **2010**, *53* (15), 5422–5438.
- (26) Amb, C. M.; Rasmussen, S. C. 6,6'-Dibromo-4,4'-Di(Hexoxymethyl)-2,2'-Bipyridine: A New Solubilizing Building Block for Macromolecular and Supramolecular Applications. *J. Org. Chem.* **2006**, *71* (12), 4696–4699.
- (27) Ariza, X.; Urpí, F.; Viladomat, C.; Vilarrasa, J. One-Pot Conversion of Azides to Boc-Protected Amines with Trimethylphosphine and Boc-ON. *Tetrahedron Lett.* **1998**, *39* (49), 9101–9102.
- (28) Ariza, X.; Urpí, F.; Vilarrasa, J. A Practical Procedure for the Preparation of Carbamates from Azides. *Tetrahedron Lett.* **1999**, *40* (42), 7515–7517.
- (29) Elmkaddem, M. K.; Fischmeister, C.; Thomas, C. M.; Renaud, J.-L. Efficient

Synthesis of Aminopyridine Derivatives by Copper Catalyzed Amination Reactions.

Chem. Commun. **2010**, *46* (6), 925–927.

(30) Schiebel, J.; Gaspari, R.; Sandner, A.; Ngo, K.; Gerber, H. D.; Cavalli, A.;

Ostermann, A.; Heine, A.; Klebe, G. Charges Shift Protonation: Neutron Diffraction

Reveals That Aniline and 2-Aminopyridine Become Protonated Upon Binding to

Trypsin. *Angew. Chemie - Int. Ed.* **2017**, *56* (17), 4887–4890.

(31) Fukada, H.; Takahashi, K. Enthalpy and Heat Capacity Changes for the Proton

Dissociation of Various Buffer Components in 0.1 M Potassium Chloride. *Proteins*

Struct. Funct. Genet. **1998**, *33* (2), 159–166.

(32) Goldberg, R. N.; Kishore, N.; Lennen, R. M. Thermodynamic Quantities for the

Ionization Reactions of Buffers. *J. Phys. Chem. Ref. Data* **2002**, *31* (2), 231–370.

(33) Dullweber, F.; Stubbs, M. T.; Musil, D.; Stürzebecher, J.; Klebe, G. Factorising

Ligand Affinity: A Combined Thermodynamic and Crystallographic Study of Trypsin

and Thrombin Inhibition. *J. Mol. Biol.* **2001**, *313* (3), 593–614.

- (34) Czodrowski, P.; Sotriffer, C. A.; Klebe, G. Protonation Changes upon Ligand Binding to Trypsin and Thrombin: Structural Interpretation Based on pK_a Calculations and ITC Experiments. *J. Mol. Biol.* **2007**, *367* (5), 1347–1356.
- (35) Baum, B.; Muley, L.; Heine, A.; Smolinski, M.; Hangauer, D.; Klebe, G. Think Twice: Understanding the High Potency of Bis(Phenyl)Methane Inhibitors of Thrombin. *J. Mol. Biol.* **2009**, *391* (3), 552–564.
- (36) Baum, B.; Muley, L.; Smolinski, M.; Heine, A.; Hangauer, D.; Klebe, G. Non-Additivity of Functional Group Contributions in Protein-Ligand Binding: A Comprehensive Study by Crystallography and Isothermal Titration Calorimetry. *J. Mol. Biol.* **2010**, *397* (4), 1042–1054.
- (37) Biela, A.; Sielaff, F.; Terwesten, F.; Heine, A.; Steinmetzer, T.; Klebe, G. Ligand Binding Stepwise Disrupts Water Network in Thrombin: Enthalpic and Entropic Changes Reveal Classical Hydrophobic Effect. *J. Med. Chem.* **2012**, *55* (13), 6094–6110.
- (38) Sandner, A.; Hu, T.; Heine, A.; Steinmetzer, T.; Klebe, G.; Weg, M. Strategies for

- Late-Stage Optimization: Profiling Thermodynamics by Preorganization and Salt Bridge Shielding. *J. Med. Chem.* **2019**, *62*, 9753–9771.
- (39) Ladbury, J. E.; Klebe, G.; Freire, E. Adding Calorimetric Data to Decision Making in Drug Development: A Hot Tip! *Nat. Rev. Drug Discov.* **2010**, *9* (1), 23–27.
- (40) Sigurskjold, B. W. Exact Analysis of Competition Ligand Binding by Displacement Isothermal Titration Calorimetry. *Anal. Biochem.* **2000**, *277* (2), 260–266.
- (41) Turnbull, W. B.; Daranas, A. H. On the Value of c : Can Low Affinity Systems Be Studied by Isothermal Titration Calorimetry? *J. Am. Chem. Soc.* **2003**, *125* (48), 14859–14866.
- (42) Page, M. J.; Macgillivray, R. T. A.; Di Cera, E. Determinants of Specificity in Coagulation Proteases. *J. Thromb. Haemost.* **2005**, *3* (11), 2401–2408.
- (43) Di Cera, E.; Guinto, E. R.; Vindigni, A.; Dang, Q. D.; Ayala, Y. M.; Wuyi, M.; Tulinsky, A. The Na^+ Binding Site of Thrombin. *J. Biol. Chem.* **1995**, *270* (38), 22089–22092.

- (44) Zhang, E.; Tulinsky, A. The Molecular Environment of the Na⁺ Binding Site of Thrombin. *Biophys. Chem.* **1997**, *63*, 185–200.
- (45) Huntington, J. A. How Na⁺ Activates Thrombin - A Review of the Functional and Structural Data. *Biol. Chem.* **2008**, *389*, 1025–1035.
- (46) Schiebel, J.; Gaspari, R.; Wulsdorf, T.; Ngo, K.; Sohn, C.; Schrader, T. E.; Cavalli, A.; Ostermann, A.; Heine, A.; Klebe, G. Intriguing Role of Water in Protein-Ligand Binding Studied by Neutron Crystallography on Trypsin Complexes. *Nat. Commun.* **2018**, *9*(1), 3559.
- (47) Stürzebecher, J.; Stürzebecher, U.; Vieweg, H.; Wagner, G.; Hauptmann, J.; Markwardt, F. Synthetic Inhibitors of Bovine Factor Xa and Thrombin Comparison of Their Anticoagulant Efficiency. *Thromb. Res.* **1989**, *54*(3), 245–252.
- (48) Gottlieb, H. E.; Kotlyar, V.; Nudelman, A. NMR Chemical Shifts of Common Laboratory Solvents as Trace Impurities. *J. Org. Chem.* **1997**, *62*(21), 7512–7515.
- (49) Schönherr, D.; Wollatz, U.; Haznar-Garbacz, D.; Hanke, U.; Box, K. J.; Taylor, R.;

- Ruiz, R.; Beato, S.; Becker, D.; Weitschies, W. Characterisation of Selected Active Agents Regarding pK_a Values, Solubility Concentrations and pH Profiles by SiriusT3. *Eur. J. Pharm. Biopharm.* **2015**, *92*, 155–170.
- (50) Keller, S.; Vargas, C.; Zhao, H.; Piszczek, G.; Brautigam, C. A.; Schuck, P. High-Precision Isothermal Titration Calorimetry with Automated Peak-Shape Analysis. *Anal. Chem.* **2012**, *84*, 5066–5073.
- (51) Scheuermann, T. H.; Brautigam, C. A. High-Precision, Automated Integration of Multiple Isothermal Titration Calorimetric Thermograms: New Features of NITPIC. *Methods* **2015**, *76*, 87–98.
- (52) Kabsch, W. Integration, Scaling, Space-Group Assignment and Post-Refinement. *Acta Crystallogr. Sect. D Biol. Crystallogr.* **2010**, *66* (2), 133–144.
- (53) Sparta, K. M.; Krug, M.; Heinemann, U.; Mueller, U.; Weiss, M. S. XDSAPP2.0. **2016**, 1085–1092.
- (54) McCoy, A. J.; Grosse-Kunstleve, R. W.; Adams, P. D.; Winn, M. D.; Storoni, L. C.;

- Read, R. J. Phaser Crystallographic Software. *J. Appl. Crystallogr.* **2007**, *40*, 658–674.
- (55) Adams, P. D.; Afonine, P. V.; Bunkóczi, G.; Chen, V. B.; Davis, I. W.; Echols, N.; Headd, J. J.; Hung, L. W.; Kapral, G. J.; Grosse-Kunstleve, R. W.; McCoy A. J.; Moriarty N. W.; Oeffner R.; Read R. J.; Richardson D. C.; Richardson J. S.; Terwilliger T. C.; Zwart P.H. *PHENIX: A Comprehensive Python-Based System for Macromolecular Structure Solution. Acta Crystallogr. Sect. D Biol. Crystallogr.* **2010**, *66* (2), 213–221.
- (56) Emsley, P.; Lohkamp, B.; Scott, W. G.; Cowtan, K. Features and Development of *Coot. Acta Crystallogr. Sect. D Biol. Crystallogr.* **2010**, *66* (4), 486–501.
- (57) Laskowski, R. A.; MacArthur, M. W.; Moss, D. S.; Thornton, J. M. *PROCHECK: A Program to Check the Stereochemical Quality of Protein Structures. J. Appl. Crystallogr.* **1993**, *26*, 283–291.
- (58) Kleywegt, G. J. *MOLEMAN* - Unpublished Program; Uppsala University: Uppsala, Sweden.

- 1
2
3
4 (59) Kleywegt, G. J.; Zou, J. Y.; Kjeldgaard, M.; Jones, T. A. *International Tables for*
5
6
7 *Crystallography: Crystallography of Biological Macromolecules*; Rossmann, M. G.,
8
9
10 Arnold, E., Eds.; Kluwer Academic Publishers: Dordrecht, The Netherlands, 2001;
11
12
13
14 Vol. F.
15
16
17
18
19
20
21
22
23
24
25
26
27
28
29
30
31
32
33
34
35
36
37
38
39
40
41
42
43
44
45
46
47
48
49
50
51
52
53
54
55
56
57
58
59
60

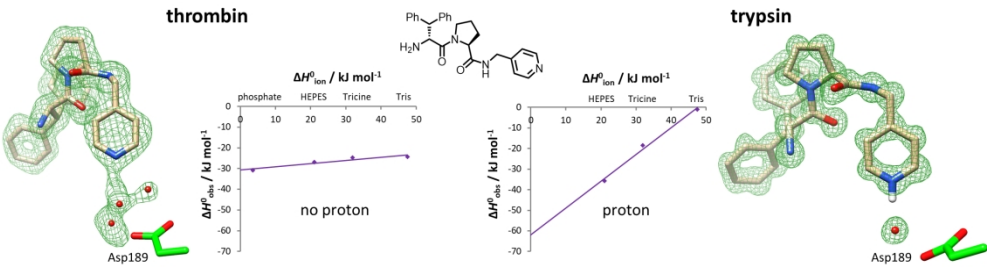


Table-of-Content Graphic

208x54mm (300 x 300 DPI)